Environmental Evaluation of the Improvements for Industrial Scaling of Zeolite Membrane Manufacturing by Life Cycle Assessment

Alberto Navajas*,†,‡, Nitish Mittal§, Neel Rangnekar§, Han Zhang§, Alfonso Cornejo†,‡, Luis M. Gandía†,‡ and Michael Tsapatsis§

Abstract

Industrial scaling of zeolite membrane manufacturing is the general aspiration of the progresses in zeolite membranes synthesis, but the evaluation of their environmental aspects has been disregarded. The objective of this study is to quantify the environmental impacts of zeolite membrane synthesis with respect to the recent advances in the synthesis of zeolite membranes: i) seed layers that allow membranes of sub-micron thickness; ii) gel-less secondary treatments that avoid the use of large amounts of expensive structure directing agents (SDA); and iii) use of low-cost polymer supports instead of conventional ceramic supports. Impacts are evaluated via life cycle assessment (LCA) which is performed using GaBi 8.7° Pro software. The impacts due to conventional and nanosheet seed layers are comparable but contribute only a small portion to the total impacts. Although the gel-less secondary growth has up to 10-fold lesser impacts compared to that for solvent-based secondary growth, Piranha-treated nanosheets method which eliminates secondary growth, can reduce impacts by an order of magnitude. It has also been found that the majority of impacts are provided by the support layer. Advancements in hollow fiber synthesis, especially using thinner fibers and less-aggressive solvents, can considerably reduce the impacts associated with overall membrane synthesis.

Keywords: Membrane synthesis methods, MFI zeolite, Environmental impact, Life Cycle Assessment

[†] Department of Applied Chemistry, Public University of Navarre, Arrosadía Campus s/n, E-31006 Pamplona, Spain

[‡] Institute for Advanced Materials (InaMat), Public University of Navarre, Arrosadía Campus s/n, E-31006 Pamplona, Spain

[§] Department of Chemical Engineering and Materials Science, University of Minnesota, 421 Washington Avenue SE, Minneapolis, MN 55455-0132, United States

^{*} Corresponding Author: e-mail address: <u>alberto.navajas@unavarra.es</u>. Telephone: (+0034) 948168444. Fax: (+0034) 948169606

Introduction

Inorganic membranes such as those fabricated from zeolites (crystalline, hydrated aluminosilicates possessing regular microporous structures) are attractive because of their high selectivity and excellent thermal, mechanical, and chemical stability. In recent years, the field of zeolite membranes has been widely reviewed¹⁻⁴. Several separations have been demonstrated at lab-scale for applications currently accomplished using energy-intensive processes such as distillation⁵⁻¹⁰. Among different zeolites, MFI-zeolite, due to their 5.5 Å multidimensional channels, has drawn attention as a material for potential membrane separations, such as butane and xylene isomer separations^{11,12}. The MFI pure silica form, silicalite-1, is highly hydrophobic and holds promise in alcohol-water separation^{13,14}.

During the last 5 years, significant progress has been made in the synthesis of zeolite membranes^{11,15-17} and their techno-economic modeling for energy savings and breakeven cost evaluation for butane isomer separation and bioethanol enrichment^{18,19}. MFI membranes have been successfully synthesized with high reproducibility and control of microstructure by secondary growth of seed layers deposited on various supports^{12,15,16,20–23}. The progress in synthesis with the main objective of industrial scaling has been mainly focused on three different aspects of the zeolite membranes:

- *Seed layer synthesis.* Discrete, intact, non-aggregated zeolite nanosheets (synthesized from the precursor multi-lamellar MFI, or ML-MFI) are used instead of conventional silicalite-1 seed layers²⁴. This improves the outlook for industrial scaling of zeolite membranes as high aspect-ratio nanometer thick zeolite membranes can be obtained using this procedure.
- Secondary treatments with reduced amounts of structure directing agents (SDA). Secondary treatments that allow zeolite layer growth have also been improved and ensure uniformity throughout the membrane interface. Gel-less treatment has been developed to make use of smaller amounts of aqueous SDA than previously used solvent-based secondary treatments^{11,14}. Moreover, synthesis techniques that do not even require secondary growth have been demonstrated; for example, a Piranha treatment was used to remove SDA by decomposition within nanosheets to create open-pore 2-dimensional zeolite nanosheet suspensions that can be deposited on porous supports through vacuum filtration¹⁵. A variant of this approach also

- eliminates the need of energy-intensive thermal treatments and the complex melt compounding process used for nanosheet exfoliation.
- suitable and low-cost support. Conventionally, ceramic supports, such as silica and alumina, have been used for zeolite membranes¹¹. Recently, polymeric (porous polybenzimidazole or PBI) support has been shown to be compatible with nanosheets prepared with the Piranha treatment method¹⁵. Other polymeric hollow supports are also expected to be appropriate if calcination is not required²⁵. This improves industrial aspects because of low cost and easier processability of polymer supports.

On the other hand, it is now becoming increasingly obvious because of environmental degradation that modern chemical plants and processes can no be longer designed using only techno-economic criteria and environmental aspects must be integral part of process design^{26,27}. Therefore, despite the progresses on synthesis of zeolite membranes in the literature with the main objective of industrial scaling, a comprehensive analysis to quantify the environmental impacts of these progresses is lacking. This complete analysis must include both energy and raw materials consumptions during zeolite membrane synthesis.

Life Cycle Assessment (LCA) has become the most used tool by academia and industry to assess the environmental impacts of manufacturing processes^{28,29}. LCA has been applied to assess the environmental impacts of membrane systems for: gas separation³⁰, water treatment³¹ and alcohol purification by pervaporation^{32,33}. These studies have shown the convenience of using LCA for that purpose. However, to our knowledge, there are no previous LCA studies applied to zeolite membranes manufacture which obviously is the first step of their life cycle. The present study applies LCA for the first time to zeolite membranes synthesis and takes into account energy and raw materials consumptions.

The objective of this study is to assess the environmental impacts of zeolite membrane synthesis by LCA in relation to the following advances in the synthesis of these materials aiming at their implementation at industrial scale: i) seed layers suitable to obtain membranes of submicron thickness; ii) gel-less secondary treatments that avoid the use of large amounts of expensive structure directing agents (SDA); and iii) use of low-cost polymer supports instead of conventional ceramic supports. The study has been divided into three sections according to the different aspects of the zeolite membranes synthesis improved. GaBi 8.7® Pro software³⁴ has been used for the LCA

modeling. Inventory data of this work will be considered in a forthcoming LCA study in which zeolite membrane pervaporation and distillation will be compared as technologies for butane isomers separation and bioethanol enrichment.

Material and methods

The LCA is carried out in compliance with ISO standard³⁵ in four steps, i.e., (1) Goal and scope, (2) Life Cycle Inventory (LCI), (3) Life Cycle Impact Analysis (LCIA), and (4) Life cycle interpretation. A primary task of the first step is to identify the system boundary; in this study, only the membrane manufacturing process is considered. GaBi 8.7® Pro software has inbuilt capability to account for the environmental impacts of extraction of materials and also for the waste release and the necessary treatments. The transportation of raw materials to the manufacturing site or any other supply-chain associated with the process is beyond the scope of this study. Limits of each study are going to be detailed on each section. As a part of LCI step, data associated with the material and energy inflows and outflows during the whole cycle are collected. Geographic limits corresponding to EU-28 have been considered for most of the materials and energy processes simulated with GaBi 8.7® Pro database. While most of the common materials can be found in the GaBi 8.7® Pro database, some of the complex chemical compounds used during membrane synthesis, such as tetraethyl orthosilicate (TEOS), tetrapropylammonium hydroxide (TPAOH), polybenzimidazole (PBI), polyethylene glycol (PEG), dimethylacetamide (DMAc), polysulphone, n-methyl-2-pyrrolidone (NMP), and diquaternary ammonium surfactant (DQAS) do not exist in the database. Thus, material and energy flows for these compounds were determined using their synthesis from other chemicals that appear on GaBi 8.7® Pro database, and discussed in the Supporting Information S1. After the LCI phase, the goal of the LCIA phase is to convert the inventory results into impacts on the environment. The LCIA phase study was performed using GaBi 8.7® Pro, and 14 Environmental Impact Indicators (EIIs) were determined through the characterization methods recommended by the European Research Center³⁶. Table S2 in Supporting Information (SI) compiles all the 14 EIIs used, the methods used for their calculation, their units and recommended level. The recommended characterization models and associated characterization factors are classified according to their quality into three levels: level "I" (recommended and satisfactory), level "II" (recommended but in need of some improvements) or

level "III" (recommended, but to be applied with caution). Finally, the results are interpreted based on values of the indicators and their comparison for various methods of membrane synthesis.

Results and discussion

Environmental impacts quantification of seed layer synthesis

The objective of this section is to compare the environmental impacts of the two most common methods for preparing of MFI-zeolite seed layer on the substrate, i.e., conventional seed layer synthesized using silica nanoparticles¹⁴ vs. nanosheet seed layer obtained by dispersible exfoliation of multilamellar MFI (ML-MFI) nanosheets²⁴. Here, only the impact associated with seed layer is considered; the impact of the secondary growth and the support layer are described in sections below. So, the functional unit of the study is the preparation of MFI- zeolite seed layer on the substrate. Data for laboratory scale synthesis (disc membrane with a total area of 3.8 cm²) are collected and scaled-up to 1,000 m² which is the order of area required for commercial implementation as discussed in techno-economic studies for butane isomer¹⁸ and ethanol/water¹⁹ separations. These are two of the most promising industrial applications of zeolite membranes as substitute of distillation. More techno-economic simulations are necessary to calculate membrane areas required for commercial implementation of other applications (e.g. gas separation, water purification).

Figure 1a shows the SEM image of the silica support after conventional seeding process and before the secondary growth. With this image it's possible to calculate a packing factor of 0.84; with seeds dimensions (2 μm x 0.8 μm x 3 μm), and considering monolayer it's possible to calculate seeds mass over 3.8 cm² support: 0.45 mg of conventional silicalite-1 seeds. Figure 1b shows membrane sketch of the nanosheet seed-based membranes. With 100 nm thick nanosheet seed layer, occupational volume fraction of nanosheets of 0.9, and MFI density of 1760 kg/m3, ML-MFI nanosheets mass at laboratory scale over the support can be calculated: 0.06 mg. Supporting Information S2 presents a discussion of the synthesis methods al laboratory scale of the seed layers. Figures S1 and S2 in SI show laboratory scale synthesis processes and the limits of the LCA study. Further, these inputs are calculated for a membrane area of 1,000 m² and Table 1 presents energy and mass inputs for the seeds layers synthesis at industrial scale.

Based on these data, different EIIs were obtained using GaBi 8.7® Pro. **Tables S3** and **S4** show the numerical values of all the EIIs for conventional and nanosheet seed layer synthesis.

Figure 2 presents a comparison of the normalized impacts of the two processes. Despite smaller quantity of silica material used in the nanosheet seed layer synthesis method, it has comparable impacts to that of conventional seed layer. This can be attributed to the use of toluene and polystyrene during ML-MFI nanosheets exfoliation and purification²² which contribute to above 70 % of the total impacts of the nanosheet seed synthesis method (**Table S4**). As the membrane synthesis from nanosheet seed layer has a better outlook for industrial scaling than those synthesized from conventional seeds, advancement in exfoliation and purification methods will further improve the environmental impact³⁷. Monte Carlo analysis (100 simulations) has been carried out to assess whether results are significantly different due to the uncertainties on data taken from laboratory and simulations³⁸. Uncertainty distributions of ± 10 % have been applied for the inputs of the processes (TEOS, TPAOH, silica, energy, polyacrylic acid, water and ethylene glycol for conventional seeds layer, and toluene, polystyrene, surfactant, ethanol, TEOS and energy for ML-MFI nanosheet seed layer). **Tables S5 and S6** show coefficients of variation (CV) of the different environmental indicators after Monte Carlo Analysis for conventional seed and nanosheet seed layers. The CV shows the variability brought about in each impact category by the risk parameters³⁹. Only inputs that introduce enough uncertainty to increase CVs values of the different EIIs above 0.3% are presented. Highest CVs are obtained for toluene in nanosheet seed layer (Human Toxicity Cancer and Eco-toxicity Freshwater indicators) because of the high incidence of the selected risk parameters in these impact categories. In any case, as the differences between the environmental indicators between both methods of seed layer preparation are so great for these EIIs (Figure 2), toluene data used in the ML-MFI exfoliation and purification does not introduce enough uncertainty for the variation of final conclusions of this section.

Environmental impacts quantification of secondary growth methods

For both the seed layers, i.e. nanosheet and conventional seeds, a secondary growth is essential to fill the non-selective gaps and improve the separation performance. A common method for secondary growth is the hydrothermal treatment in which the seeded substrate is immersed in an aqueous silica solution (solvent-based)²⁴ containing a structure directing agent (SDA). Although it leads to selective membranes, this method requires large amounts of chemicals. Thus, gel-less or gel-free methods of secondary growth have been developed in which the thermal treatment is performed in a closed vessel with only small amount of aqueous solution^{11,12,14}. In this

section, the environmental impact associated with these different secondary growth methods is considered. So, the functional unit of the study is the growth layer from the MFI- zeolite seed layer on the substrate. **Supporting Information S3** presents a discussion of the secondary growth synthesis. **Figures S3** and **S4** show laboratory scale synthesis processes and the limits of the LCA study and **Table 2** shows the material and energy inputs for industrial scale syntheses.

Tables S7 and S8 show EIIs numerical values for the solvent-based and gel-less secondary growth methods, respectively, and Figure 3 shows a comparison of the normalized impacts of the two processes. As shown, the solvent-based secondary treatment has significantly higher EIIs than the gel-free method. This can be attributed to the 4-fold larger amount of SDA and the high amount of used in the solvent-based method (Table S7). Further, the impacts due to secondary growth are significantly higher than that of seed layer synthesis; even gel-less method has about 15-fold higher impacts than nanosheet-based seed layer method. A Monte Carlo analysis has been carried out to assess whether results are significantly different due to the uncertainties on data, and Tables S9 shows CV of the different EIIs observed. As before, only inputs that introduce enough uncertainty to increase CVs values of the different EIIs above 0.3% are presented. Highest uncertainties (CVs \geq 4.0 %) are observed in 7 EIIs due to the standard deviation introduced in gel-less secondary growth inputs. On the other hand, CVs between 3.0 % and 4.0 % are observed in 11 of the 14 EIIs due to the standard deviation introduced in TEOS solvent-based secondary growth input. However, as the differences between the values of the EIIs for both secondary growth methods are so marked (Figure 3), the uncertainties introduced by these input data do not vary the final conclusions of the analysis.

Recently, Zhang et al.¹⁵ developed an innovative technique that does not require any secondary growth. In this method, selective membranes were obtained by filter-coating Piranhatreated open-pore nanosheets over porous PBI support. The nanosheets prepared using this method have been successfully applied to a PBI polymer support. Since, the resulting membranes did not show as high selectivity as membranes after secondary growth, they hold promise only for certain applications that do not require high selectivity¹⁸. However, further improvements in nanosheet coating quality may enable more demanding uses. An additional feature of this method is that it does not require any calcination to remove the SDA from the zeolite pores. Instead, a Piranha solution (H₂SO₄/H₂O₂ 3:1, v/v) is used to remove the SDA from the nanosheets before coating them on the support. This synthesis method is presented in the **Supporting Information S4** and

Figure S5 shows laboratory scale synthesis processes and the limits of the LCA study. Table 3 presents the material and energy inputs for industrial scale syntheses. Since membranes are prepared without any secondary growth, the impact of this method is compared to the combined impact of the seed layer synthesis and secondary growth. The functional unit of the study is the the preparation of Piranha-treated open-pore nanosheets. Nanosheet seed layer and gel-less secondary growth methods have been considered for comparison (Figure S6). Table S10 shows EIIs numerical values for the Piranha treated nanosheets method and Figure 4 presents a comparison of the normalized impacts of the two processes. Although strong acid is contained by the Piranha solution, the Piranha-treated nanosheets method is found to have lower impact as it eliminates the secondary growth, which has about 10-fold impact as compared to the ML-MFI nanosheet synthesis. Thus, this method has considerable potential for reducing environmental impacts if the membrane performance remains satisfactory. In this aspect, although it has not been considered in this LCA study, it is worth noting that membrane synthesis reproducibility is low when strong treatments are applied to zeolite layers⁴⁰. Monte Carlo analysis reveals that the highest CVs are observed for Ozone Layer Depletion (ODP) and Ionization Radiation (IR) indicators due to uncertainties in TEOS, and for Human Toxicity Non-Cancer (HTNC) indicator in DQAS (Table S11). However, Figure 4 shows so marked differences between the values of these EIIs for both secondary growth methods, that the uncertainties introduced by these input data do not vary the final conclusions of the analysis.

Environmental impacts quantification of support synthesis

The seed layer and secondary growth methods analyzed in the previous sections have been used with several supports in order to build robust membranes. Silica and alumina support substrates have been used with both methods^{11,14,24}. While silica can be used for both solvent-based and gel-free secondary growth, alumina is restricted only to solvent-based methods as its use has not been demonstrated for the former. Furthermore, PBI polymer supports have been used for Piranha-treated nanosheets membranes¹⁵. The objective of this section is to compare the environmental impacts associated with manufacturing of all three kinds of supports on an industrial scale and because of this the functional unit is the membrane support manufacture.

Supporting Information S5 presents a discussion for the synthesis of various supports and **Figures S7** and **S8** show silica and PBI laboratory scale synthesis processes and the limits of

the LCA study. **Table 4** shows material and energy inputs for different support synthesis methods for a membrane area of 1,000 m².

Tables S12, S13 and S14 show EIIs numerical values for the three supports synthesis methods at industrial scale, respectively. The support synthesis process has significantly higher impacts than the seed layer and secondary growth methods. Further, Figure 5 presents a comparison of the normalized impact of the three kinds of support. It can be seen that silica support has the highest impacts followed by alumina and PBI support. It should be noted that 3 mm thick supports are considered for both silica and alumina resulting in similar requirement of glass wool (4.4 kg/m²) and alumina (5.2 kg/m²) for the support synthesis. In spite of the similar amounts, the impacts of silica support are up to 5-fold higher than those of alumina due to the difference in the impacts associated with the manufacture of quartz-wool and alumina which contribute to above 90 % of the total impact. The impacts of PBI support are significantly lower than for both the silica (about 50-fold lower) and alumina (about 10-fold lower) supports. This is because only a 370 μm thick PBI support is considered, which results in a very low amount of PBI material. Further, these impacts contribute 70 % to the total impacts, increasing the contribution of those associated to the solvents used in the process as compared to that for silica or alumina supports where the material contributes to about 90 % of the impacts. Monte Carlo analysis shows that the main CVs (Table S15) comes from quartz-wool, alumina, and PBI manufacture processes on the silica, alumina and PBI supports, respectively. The source of data uncertainty may come from the amount used of each compound or from the simulation used in their manufacture³⁸. Quartz-wool, alumina and PBI amounts were directly obtained from laboratory (Supporting information S5) and extrapolated to industrial scale (Table 4). Quartz-wool manufacture process is in-built in GaBi 8.7® Pro database⁴¹, alumina inputs and outputs inventory have been obtained from the last environmental profile of the European Aluminium⁴², and PBI manufacture process has been simulated following procedure described in detail in Supporting Information S1.3. Both amounts data and simulations done are reliable and conclusions of this analysis are robust.

Recently, zeolite membranes of 5 µm thickness over hollow-fiber alumina supports have been fabricated⁴³. **Supporting Information S5.4** presents a discussion of the alumina hollow fiber synthesis and **Table S16** shows the corresponding impacts. The hollow fiber supports have lesser impacts as compared to flat alumina supports due to thinner and more porous fibers making these comparable to the PBI supports (**Figure 6**). Monte Carlo analysis shows that alumina and N-

methyl-2-pyrrolidone used during HF alumina manufacture are the main sources of uncertainty (**Table S15**). Amounts of each compound at laboratory scale were directly obtained from literature⁴³ (**Supporting information S5.4**) and extrapolated to industrial scale (**Table 4**). Regarding their simulations, N-methyl-2-pyrrolidone synthesis was explained in **Supporting Information S1.7**, and as above, alumina has been simulated following literature⁴². Both amounts data and simulations done are reliable and conclusions of this analysis robust.

Although hollow fibers support is better suited for commercialization due to their higher packing density, it is worth noting that depending on the selective membrane layer thickness the external diameter of the fibers can be higher and the packing density can decrease. It should also be noted that as recent studies demonstrate, the preparation of selective zeolite and metalorganic hollow fibers is not obvious⁴⁴⁻⁴⁷. However, thinner hollow fibers combined with less-aggressive solvents usage should be explored to further reduce the environmental impacts of membrane manufacturing.

Conclusions

It has been carried out LCAs of several synthesis methods of zeolite membranes in order to know if progresses in zeolite membrane synthesis reduce environmental impacts as well as improve industrial scaling outlook; conventional nanoparticles and exfoliated nanosheets for seed layer synthesis, sol-gel and gel-less methods for secondary growth, and alumina, silica and polymer-based supports are explored. Although conventional seeds and nanosheet seeds have comparable impacts, their impacts are negligible as compared to the impacts of secondary treatments and supports synthesis. Substitution of secondary growth by vacuum filtration of Piranha-treated nanosheets on PBI support is found to have significantly lesser impacts due to the elimination of secondary growth process. The major contribution to the impacts is provided by the support preparation. For alumina and silica flat supports which are about 3 mm in thickness, a major portion of impacts is associated with the support material itself. These impacts can be reduced by either using PBI polymer support and/or using thinner hollow fiber supports. While the impacts of the hollow fiber supports are comparable to that of the combined impacts of nanosheet seed and gel-less secondary growth methods, the support contributes to more than 90 % of the impacts when compared to the Piranha-treated open-pore nanosheet-based method. Thus,

advancements in hollow fiber synthesis, especially using thinner fibers and less-aggressive solvents, can considerably reduce the impacts associated with membrane preparation.

Supporting Information

Environmental impacts indicators used, Life Cycle Inventory of complex chemical compounds, seed layer synthesis, secondary treatments methods, and support synthesis inventories, limits and flowcharts, Environmental impacts indicators results, and Monte Carlo Coefficients of Variation.

Acknowledgements

MT acknowledges support from the National Science Foundation, Division of Chemical, Bioengineering, Environmental and Transport Systems under award number CBET 1705687.

References

- (1) Caro, J.; Noack, M. Zeolite membranes Recent developments and progress. *Micropor. Mesopor. Mater.* **2008**, *115*, 215–233.
- (2) Rangnekar, N.; Mittal, N.; Elyassi, B.; Caro, J.; Tsapatsis, M. Zeolite membranes a review and comparison with MOFs. *Chem. Soc. Rev.* **2015**, *44*, 7128–7154.
- (3) Gascon, J.; Kapteijn, F.; Zornoza, B.; Sebastián, V.; Casado, C.; Coronas, J. Practical approach to zeolitic membranes and coatings: State of the art, opportunities, barriers, and future perspectives. *Chem. Mater.* **2012**, *24*, 2829–2844.
- (4) Pina, M.P.; Mallada, R.; Arruebo, M.; Urbiztondo, M.; Navascués, N.; de la Iglesia, O.; Santamaria, J. Zeolite films and membranes. Emerging applications. *Micropor. Mesopor. Mater.* **2011**, *144*, 19–27.
- (5) Pera-Titus, M. Porous Inorganic Membranes for CO ₂ Capture: Present and Prospects. *Chem. Rev.* **2014**, *114*, 1413–1492.
- (6) Kosinov, N.; Gascon, J.; Kapteijn, F.; Hensen, E.J.M. Recent developments in zeolite membranes for gas separation. *J. Membrane Sci.* **2016**, *499*, 65–79.
- (7) Yuan, W.; Lin, Y.S.; Yang, W. Molecular Sieving MFI-Type Zeolite Membranes for Pervaporation Separation of Xylene Isomers. *J. Am. Chem. Soc.* **2004**, *126*, 4776–4777.
- (8) Nikolakis, V.; Xomeritakis, G.; Abibi, A.; Dickson, M.; Tsapatsis, M. Vlachos, D.G.; Growth of a faujasite-type zeolite membrane and its application in the separation of saturated/unsaturated hydrocarbon mixtures. *J. Membrane Sci.* **2001**, *184*, 209–219.
- (9) Morigami, Y.; Kondo, M.; Abe, J.; Kita, H.; Okamoto, K. The first large-scale pervaporation plant using tubular-type module with zeolite NaA membrane. *Sep. Purif. Technol.* **2001,** *25*, 251–260.
- (10) Tomita, T.; Nakayama, K.; Sakai, H. Gas separation characteristics of DDR type zeolite membrane. *Micropor. Mesopor. Mater.* **2004,** *68,* 71–75.
- (11) Agrawal, K.V.; Topuz, B.; Pham, T.C.T.; Nguyen, T.H.; Sauer, N.; Rangnekar, N.; Zhang, H.; Narasimharao, K.; Basahel, S.N.; Francis, L.F.; Macosko, C.W.; Al-Thabaiti, S.; Tsapatsis, M.; Yoon, K.B. Oriented MFI membranes by gel-less secondary growth of sub-100 nm MFI-nanosheet seed layers. *Adv. Mater.* **2015**, *27*, 3243–3249.
- (12) Pham, T.C.T.; Nguyen, T.H.; Yoon, K.B. Gel-free secondary growth of uniformly oriented silica MFI zeolite films and application for xylene separation. *Angew. Chem. Int. Edit.* **2013**, *52*, 8693–8698.
- (13) Zhou, H.; Korelskiy, D.; Sjöberg, E.; Hedlund, J. Ultrathin hydrophobic MFI membranes. *Micropor. Mesopor. Mater.* **2014**, *192*, 76–81.

- (14) Elyassi, B.; Jeon, M.Y.; Tsapatsis, M.; Narasimharao, K.; Sulaiman, N.M.N.; Al-Thabaiti, S. Ethanol/Water Mixture Pervaporation Performance of b-Oriented Silicalite-1 Membranes Made by Gel-Free Secondary Growth. *AIChE J.* **2016**, *62*, 556-563.
- (15) Zhang, H.; Xiao, Q.; Guo, X.; Li, N.; Kumar, P.; Rangnekar, N.; Jeon, M.Y.; Al-Thabaiti, S.; Narasimharao, K.; Basahel, S.N.; Topuz, B.; Onorato, F.J.; Macosko, C.W.; Mkhoyan, K.A.; Tsapatsis, M. Open-Pore Two-Dimensional MFI Zeolite Nanosheets for the Fabrication of Hydrocarbon-Isomer-Selective Membranes on Porous Polymer Supports. *Angew. Chem. Int. Edit.* 2016, 55, 7184–7187.
- (16) Jeon, M.Y.; Kim, D.; Kumar, P.; Lee, P.S.; Rangnekar, N.; Bai, P.; Shete, M.; Elyassi, B.; Lee, H.S.; Narasimharao, K.; Basahel, S.N.; Al-Thabaiti, S.; Xu, W.; Cho, H.J.; Fetisov, E.O.; Thyagarajan, R.; DeJaco, R.F.; Fan, W.; Mkhoyan, K.A.; Siepmann, J.I.; Tsapatsis, M. Ultra-selective high-flux membranes from directly synthesized zeolite nanosheets. *Nature* 2017, *543*, 690-694.
- (17) Rangnekar, N.; Shete, M.; Agrawal, K.V.; Topuz, B.; Kumar, P.; Guo, Q.; Ismail, I.; Alyoubi, A.; Basahel, S.; Narasimharao, K.; Macosko, C.W.; Mkhoyan, K.A.; Al-Thabaiti, S.; Stottrup, B.; Tsapatsis, M. 2D zeolite coatings: Langmuir-Schaefer deposition of 3 nm thick MFI zeolite nanosheets. *Angew. Chem. Int. Edit.* **2015**, *54*, 6571–6575.
- (18) Mittal, N.; Bai, P.; Kelloway, A.; Siepmann, J.I.; Daoutidis, P.; Tsapatsis, M. A mathematical model for zeolite membrane module performance and its use for technoeconomic evaluation of improved energy efficiency hybrid membrane-distillation processes for butane isomer separations. *J. Membrane Sci.* **2016**, *520*, 434–449.
- (19) Mittal, N.; Bai, P.; Siepmann, J.I.; Daoutidis, P.; Tsapatsis, M. Bioethanol enrichment using zeolite membranes: Molecular modeling, conceptual process design and techno-economic analysis. *J. Membrane Sci.* **2017**, *540*, 464–476.
- (20) Lai, Z.; Bonilla, G.; Diaz, I.; Nery, J.G.; Sujaoti, K.; Amat, M.A.; Kokkoli, E.; Terasaki, O.; Thompson, R.W.; Tsapatsis, M.; Vlachos, D.G. Microstructural optimization of a zeolite membrane for organic vapor separation, *Science* **2003**, *300*, 456–460.
- (21) Liu Y.; Li, Y.; Cai, R.; Yang, W. Suppression of twins in b-oriented MFI molecular sieve films under microwave irradiation. *Chem. Commun.* **2012**, *48*, 6782-6784.
- (22) Liu, Y.; Li, Y.; Yang, W. Fabrication of Highly *b*-Oriented MFI Film with Molecular Sieving Properties by Controlled In-Plane Secondary Growth. *J. Am. Chem. Soc.* **2010**, *132*, 1768–1769.
- (23) Wang, H.; Dong, X.; Lin, Y.S. Highly stable bilayer MFI zeolite membranes for high temperature hydrogen separation. *J. Membrane Sci.* **2014,** *450,* 425-432.
- (24) Varoon, K.; Zhang, X.; Elyassi, B.; Brewer, D.D.; Gettel, M.; Kumar, S.; Lee, J.A.; Maheshwari, S.; Mittal, A.; Sung, C.Y.; Cococcioni, M.; Francis, L.F.; McCormick, A.V.; Mkhoyan, K.A.; Tsapatsis, M. Dispersible exfoliated zeolite nanosheets and their application as a selective membrane. *Science* **2011**, *334*, 72–75.

- (25) Zhana, Z.; Shao, J.; Peng, Y.; Wang, Z.; Yan, Y. High performance zeolite NaA membranes synthesized on the inner surface of zeolite/PES-PI blend composite hollow fibers. *J. Membrane Sci.* **2014**, *471*, 299-307.
- (26) Azapagic, A.; Perdan, S. Sustainable Chemical Engineering: Dealing with "Wicked" Sustainability Problems. *AIChE J.* **2014**, *60*, 3998–4007.
- (27) Galli, F.; Pirola, C.; Previtali, D.; Manenti, F.; Bianchi, C. L. Eco Design LCA of an Innovative Lab Scale Plant for the Production of Oxygen-Enriched Air. Comparison between Economic and Environmental Assessment. *J. Clean. Prod.* **2018**, *171*, 147–152.
- (28) Brones, F.; De Carvalho, M. M.; De Senzi Zancul, E. Ecodesign in Project Management: A Missing Link for the Integration of Sustainability in Product Development? *J. Clean. Prod.* **2014**, *80*, 106–118.
- (29) Münster, M.; Ravn, H.; Hedegaard, K.; Juul, N.; Ljunggren Söderman, M. Economic and Environmental Optimization of Waste Treatment. *Waste Manage*. **2015**, *38*, 486–495.
- (30) Giordano, L.; Roizard, D.; Favre, E. Life cycle assessment of post-combustion CO2 capture: A comparison between membrane separation and chemical absorption processes. *Int. J. Greenh. Gas Con.* **2018**, *68*, 146-163.
- (31) Martins, A. A.; Caetano, N. S.; Mata, T. M. LCA for Membrane Processes. In *Sustainable Membrane Technology for Water and Wastewater Treatment*; Figoli, A., Criscuoli, A., Eds.; Springer Singapore: Singapore, 2017; pp 23–66.
- (32) Luis, P.; Amelio, A.; Vreysen, S.; Calabro, V.; Van der Bruggen, B. Simulation and Environmental Evaluation of Process Design: Distillation vs. Hybrid Distillation-Pervaporation for Methanol/Tetrahydrofuran Separation. *Appl. Energ.* **2014**, *113*, 565–575.
- (33) Andre, A.; Nagy, T.; Toth, A. J.; Haaz, E.; Fozer, D.; Tarjani, J. A.; Mizsey, P. Distillation Contra Pervaporation: Comprehensive Investigation of Isobutanol-Water Separation. *J. Clean. Prod.* **2018**, *187*, 804–818.
- (34) Life Cycle Assessment LCA Software: GaBi Software. http://www.gabi-software.com/america/index/ (accessed March 16, 2018).
- (35) ISO standards for life cycle assessment to promote sustainable development. https://www.iso.org/news/2006/07/Ref1019.html (accessed March 16, 2018).
- (36) Characterization factors of the ILCD recommended life cycle impact assessment methods. http://eplca.jrc.ec.europa.eu/?page_id=86 (accessed March 16, 2018).
- (37) Sabnis, S.; Tanna, V.A.; Li, C.; Zhu, J.; Vattipalli, V.; Nonnenmann, S.S.; Sheng, G.; Lai, Z.; Winter, H.H.; Fan, W. Exfoliation of two-dimensional zeolites in liquid polybutadienes,

- (38) Huijbregts, M. A. J. Application of Uncertainty and Variability in LCA. *Int. J. Life Cycle Ass.* **1998**, *3*, 273-280.
- (39) Escobar, N.; Ribal, J.; Clemente, G.; Sanjuán, N. Consequential LCA of Two Alternative Systems for Biodiesel Consumption in Spain, Considering Uncertainty. *J. Clean. Prod.* **2014**, *79*, 61–73.
- 40) Navajas, A.; Mallada, R.; Téllez, C.; Coronas, J.; Menéndez, M.; Santamaría, J. Study on the Reproducibility of Mordenite Tubular Membranes Used in the Dehydration of Ethanol. *J. Membrane Sci.* **2007**, *299*, 166-173.
- (41) ThinkStep. Process data set: Glass wool; fleece; production mix, at plant; density between 10 to 100 kg/m3. http://gabi-documentation-2018.gabi-software.com/xml-data/processes/898618b8-3306-11dd-bd11-0800200c9a66.xml (accessed March 16, 2018).
- (42) European Aluminium Association, Environmental profile report, Life-Cycle inventory data for aluminium production and transformation processes in Europe February 2018. https://www.european-aluminium.eu/resource-hub/environmental-profile-report-2018/ (accessed March 16, 2018).
- (43) Shao, J.; Zhan, Z.; Li, J.; Wang, Z.; Li, K.; Yan, Y. Zeolite NaA membranes supported on alumina hollow fibers: Effect of support resistances on pervaporation performance. *J. Membrane Sci.* **2014**, *451*, 10–17.
- (44) Brown, A.J.; Johnson, J.R.; Lydon, M.E.; Koros, W.J.; Jones, C.W.; Nair, S. Continuous Polycrystalline Zeolitic Imidazolate Framework-90 Membranes on Polymeric Hollow Fibers. *Angew. Chem. Int. Edit.* **2012**, *51*, 10615–10618.
- (45) Brown, A. J.; Brunelli, N. A.; Eum, K.; Rashidi, F.; Johnson, J. R.; Koros, W. J.; Jones, C. W.; Nair, S. Interfacial Microfluidic Processing of Metal-Organic Framework Hollow Fiber Membranes. *Science* **2014**, *345*, 72-75.
- (46) Cacho-Bailo, F.; Catalán-Aguirre, S.; Etxeberría-Benavides, M.; Karvan, O.; Sebastian, V.; Téllez, C.; Coronas, J. Metal-Organic Framework Membranes on the Inner-Side of a Polymeric Hollow Fiber by Microfluidic Synthesis. *J. Membrane Sci.* 2015, 476, 277–285.
- (47) Biswal, B. P.; Bhaskar, A.; Banerjee, R.; Kharul, U. K. Selective Interfacial Synthesis of Metal–organic Frameworks on a Polybenzimidazole Hollow Fiber Membrane for Gas Separation. *Nanoscale* **2015**, *7*, 7291–7298.

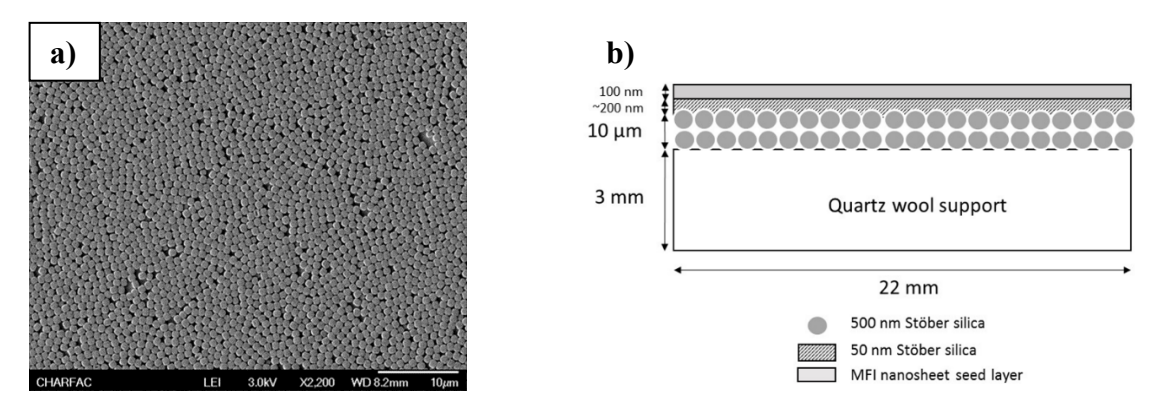


Figure 1. (a) SEM image (top-view) of silicalite-1 membrane supported on silica support before secondary growth and after seeding process using conventional nanoparticle seeds. **(b)** Schematic of silicalite-1 membrane supported on silica support before secondary growth and after 100 nm thick ML-MFI nanosheet based seeding process.

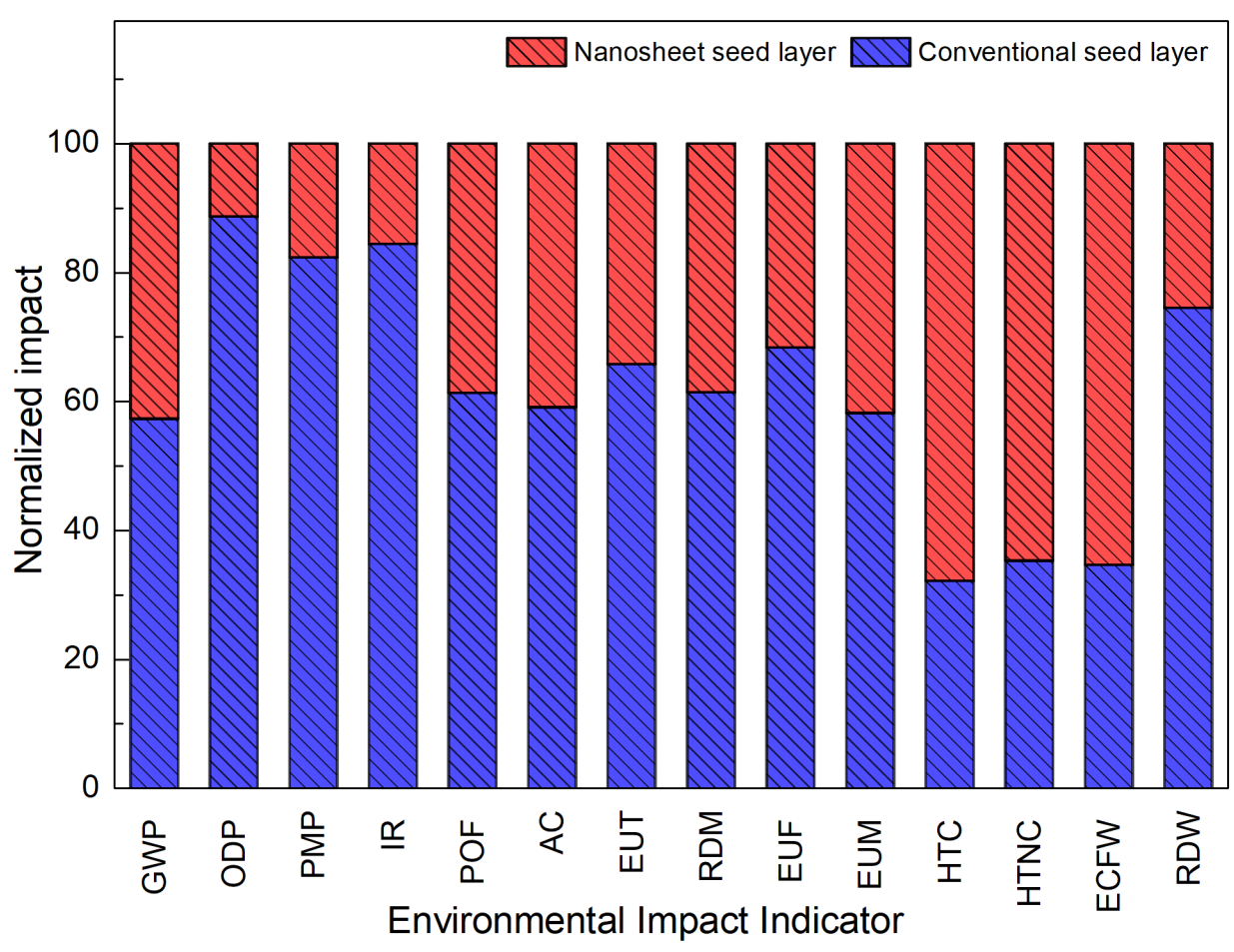


Figure 2. Comparison between the normalized impacts of nanosheet-based seed layer synthesis method and conventional nanoparticle-based seed layer synthesis methods. **Table S2** in **Supplementary information** describes the 14 EIIs, the methods used for their calculation, their units and recommended level.

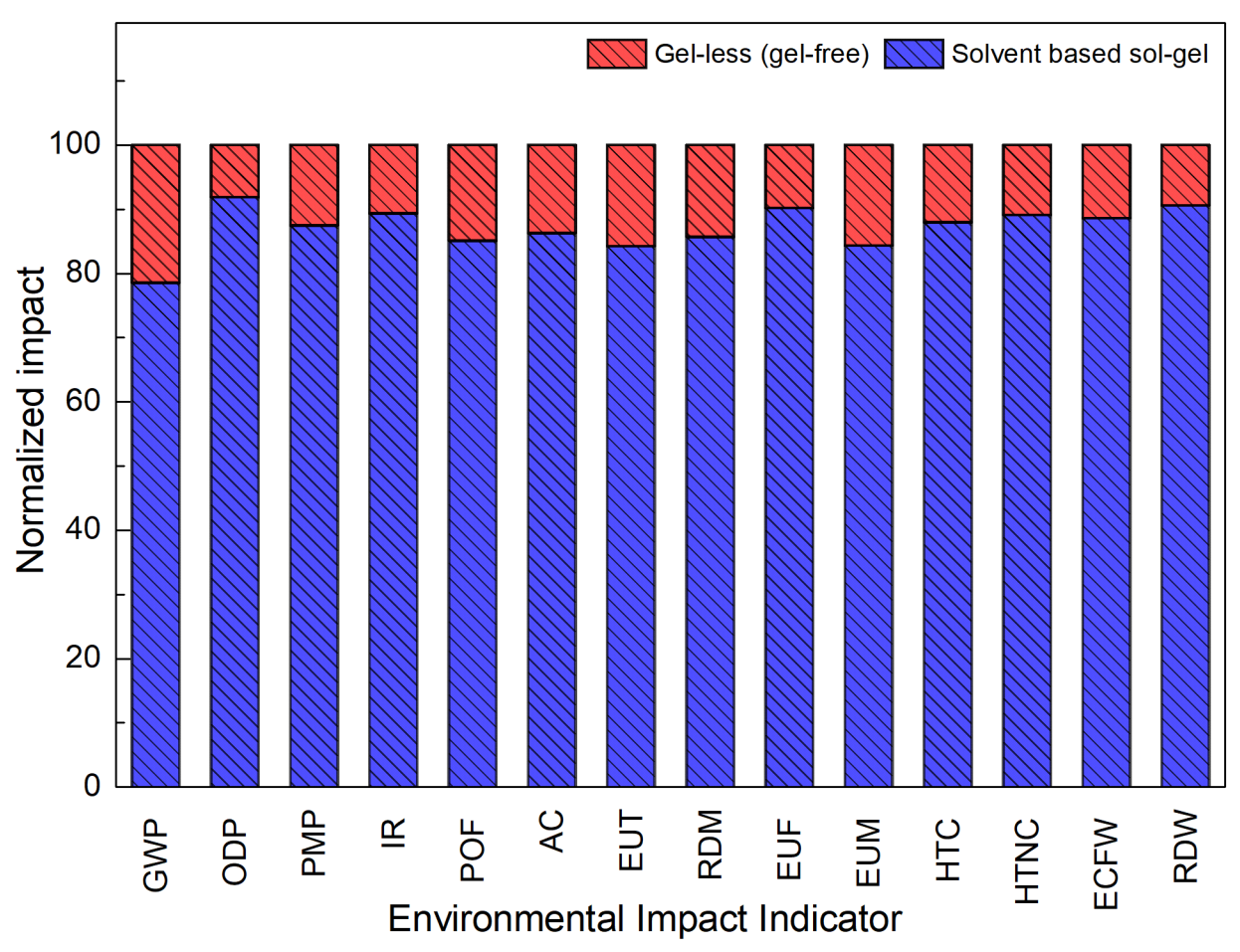


Figure 3. Comparison between the normalized impacts of gel-less secondary growth and solvent-based sol-gel secondary growth method.

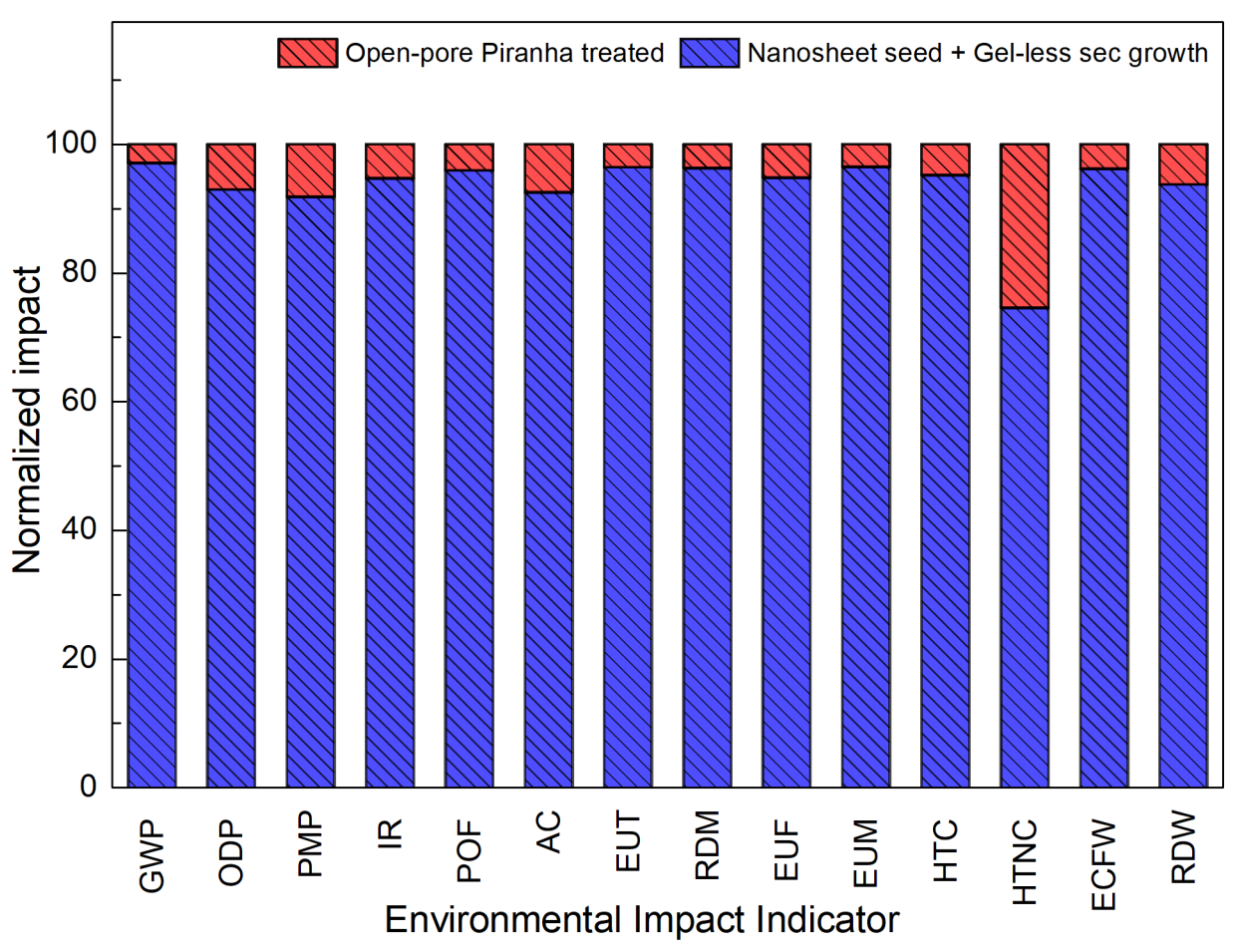


Figure 4. Comparison between the normalized impacts of Piranha-treated open-pore membrane synthesis method and combination of nanosheet-based seeding process and gel-less secondary growth method.

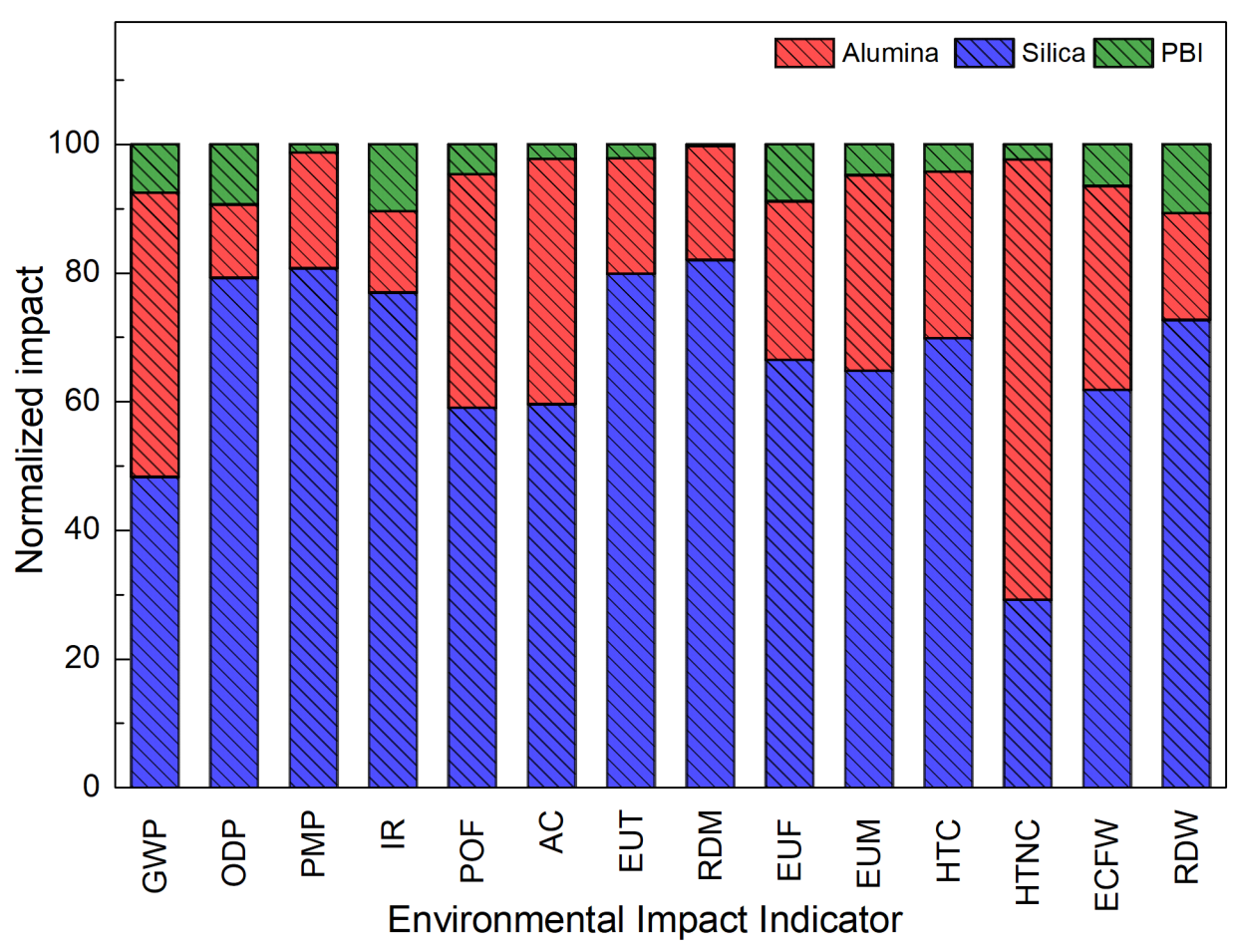


Figure 5. Comparison among the normalized impacts of different kinds of support synthesis methods: silica support, alumina support and PBI polymer support.

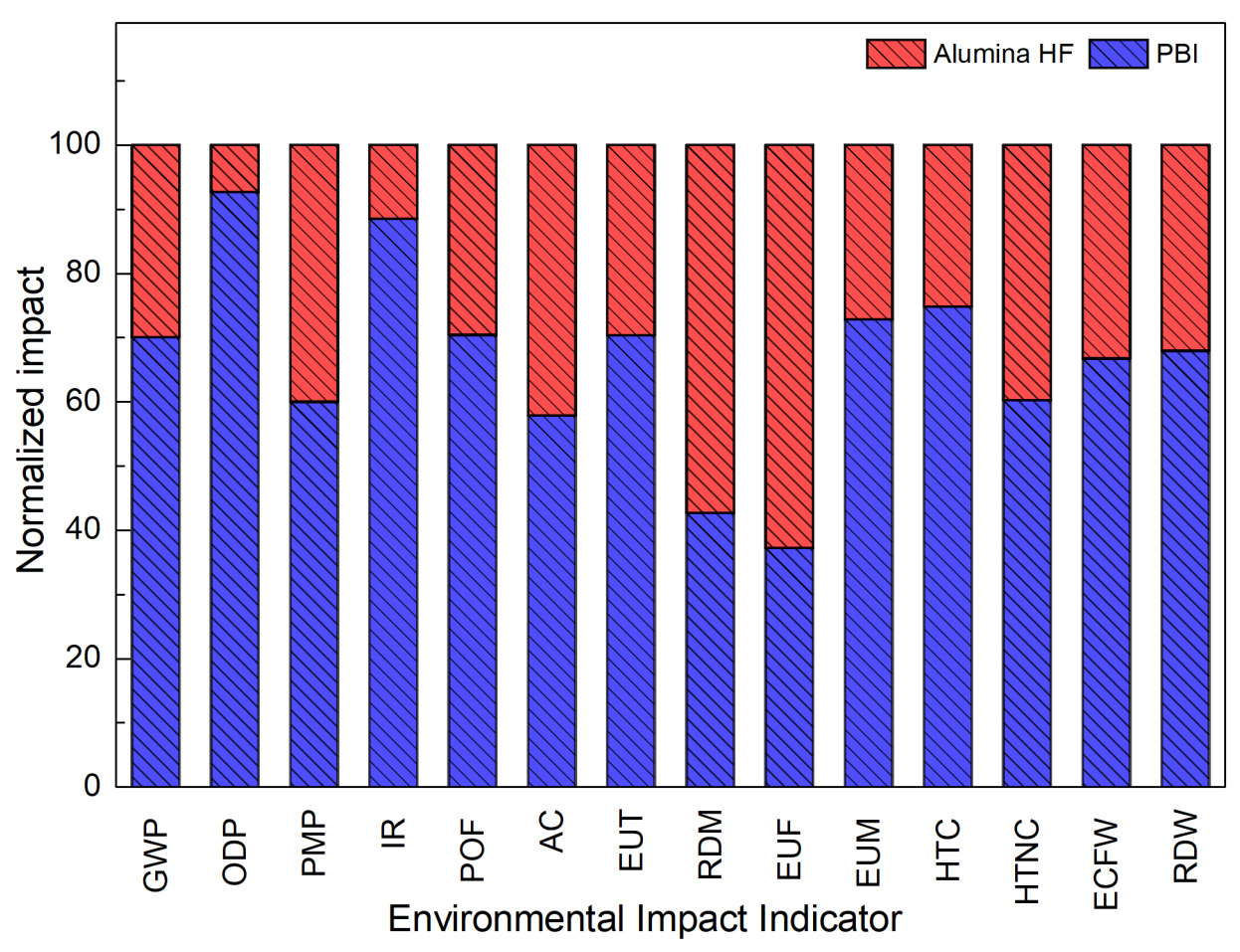


Figure 6. Comparison between the normalized impacts of alumina hollow fiber support and PBI polymer flat disc support at industrial scale synthesis methods.

Table 1. Material (gm) and energy (kWh) inputs for conventional and nanosheet seed layer synthesis for a membrane area of 1,000 m²

	Conventional seeds	ML-MFI nanosheet seeds
Tetraethyl orthosilicate	4,09E+03	5,49E+02
Tetrapropylammonium hydroxide	5,98E+02	
Silica	1,39E+03	
Water	5,12E+04	1,90E+02
Polyacrylic acid	8,97E+03	
Ethylene glycol	3,59E+03	
Diquaternary ammonium surfactant		2,38E+02
Ethanol		4,86E+01
Polystyrene		3,96E+03
Toluene		3,13E+04
Energy	8,62E+01	4,09E+01

Table 2. Material (gm) and energy (kWh) inputs for secondary growth using solvent-based and gel-free methods for a membrane area of $1,000 \text{ m}^2$

	Solvent based sol-gel	Gel-less (gel-free)
Tetraethyl orthosilicate	3,84E+05	
Tetrapropylammonium hydroxide	5,62E+04	1,34E+04
Water	2,24E+06	2,63E+06
Ethanol	1,70E+05	
Energy	3,62E+03	2,79E+03

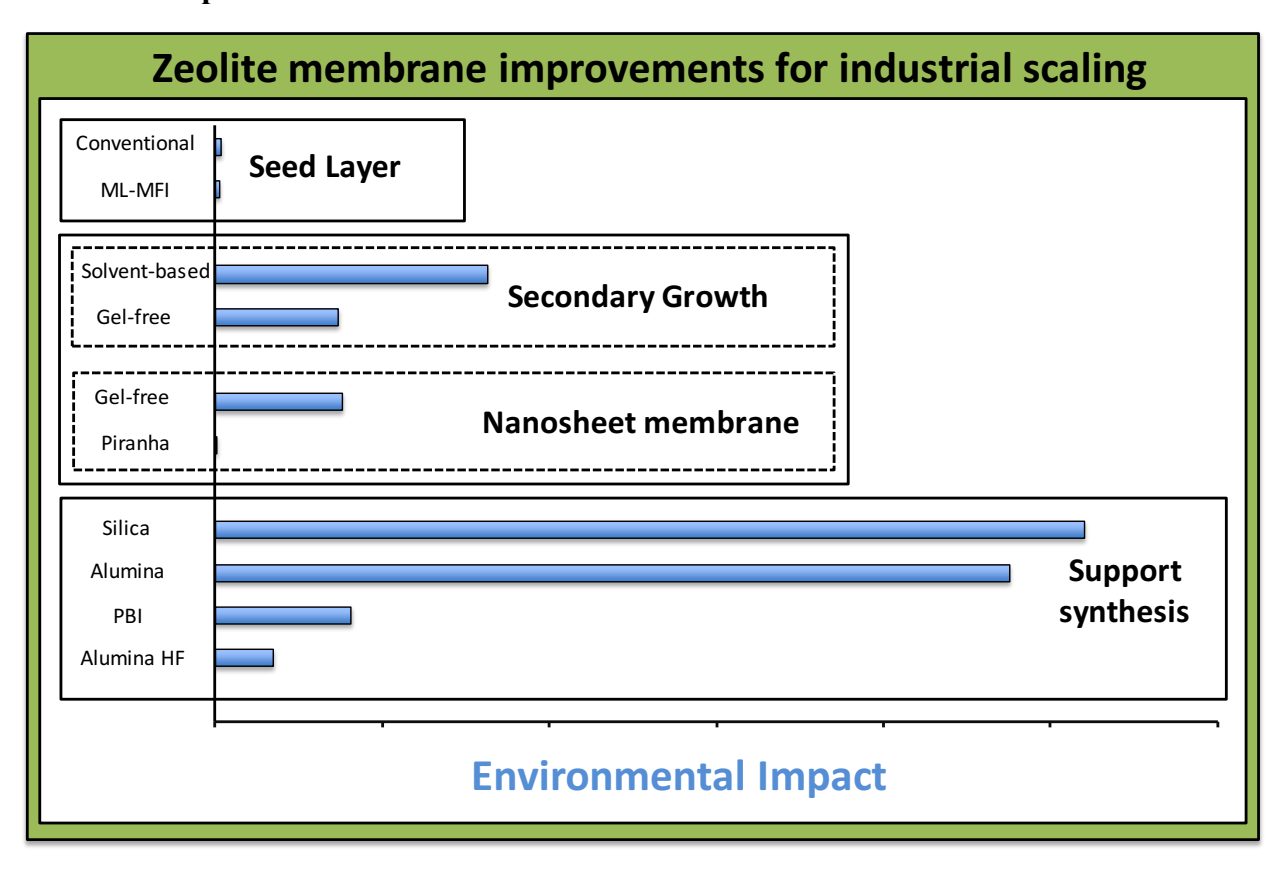
Table 3. Material (gm) and energy (kWh) inputs for Piranha-treated membrane synthesis method for a membrane area of 1,000 m²

	Piranha-treated membrane synthesis
Tetraethyl orthosilicate	2,75E+03
Diquaternary ammonium surfactant	1,19E+03
Water	2,21E+03
Ethanol	2,43E+02
Hydrogen peroxide	5,39E+02
Sulphuric acid	8,74E+03
Energy	3,48E+01

Table 4. Material (gm) and energy (kWh) inputs for several kinds of support synthesis for a membrane area of 1,000 m²

	Silica	Alumina	Alumina hollow fiber	PBI polymer
Quartz wool	4,47E+06			
Ethanol	7,24E+04			
Tetraethyl orthosilicate	6,25E+04			
Ammonia	1,77E+04			
Polyvinyl alcohol	7,89E+03			
Water	1,60E+06		8,98E+04	
Alumina		8,29E+06	1,24E+05	
n-Methyl-2-pyrrolidone			8,98E+04	
Polyethersulfone			2,08E+04	
Polyvinylpyrrolidone			1,18E+03	
Polybenzimidazole				7,91E+04
Dimethyl acetamide				4,48E+04
Polyethylene glycol				2,64E+04
Energy	7,39E+03	3,67E+03	1,81E+02	3,43E+02

Abstract Graphic



Synopsis

Improvements in zeolite membrane synthesis have better outlook for industrial scaling as well as reduce environmental impacts.

Supporting Information for:

Environmental Evaluation of the Improvements for Industrial Scaling of Zeolite Membrane Manufacturing by Life Cycle Assessment

Alberto Navajas*, †,‡ , Nitish Mittal $^{\$}$, Neel Rangnekar $^{\$}$, Han Zhang $^{\$}$, Alfonso Cornejo †,‡ , Luis M. Gandía †,‡ and Michael Tsapatsis $^{\$}$

† Department of Applied Chemistry, Public University of Navarre, Arrosadía Campus s/n, E-31006 Pamplona, Spain

[‡] Institute for Advanced Materials (InaMat), Public University of Navarre, Arrosadía Campus s/n, E-31006 Pamplona, Spain

§ Department of Chemical Engineering and Materials Science, University of Minnesota, 421 Washington Avenue SE, Minneapolis, MN 55455-0132, United States

* Corresponding Author: e-mail address: <u>alberto.navajas@unavarra.es</u>. Telephone: (+0034) 948168444. Fax: (+0034) 948169606

Number of Pages: 49

Number of Figures: 9

Number of Tables: 16

Table of Contents:

S1. Complex chemical compounds	
S1.1. Tetraethyl orthosilicate	S4
S1.2. Tetrapropylammonium hydroxide	S5
S1.3. Polybenzimidazole	S5
S1.4. Dimethylacetamide	S9
S1.5. Polyethylene Glycol	S10
S1.6. Polysulfone	S11
S1.7. N-methyl-2-pyrrolidone	S11
S1.8. Surfactant C ₂₂₋₆₋₆ (OH) ₂	S12
S2. Seed layer synthesis	
S2.1 Conventional seed layer	S13
S2.2 Multi-lamellar nanosheet seed layer	S14
S3. Secondary growth method	S15
S3.1 Solvent-based sol-gel method	S15
S3.2 Gel-less (gel-free) method	S16
S4. Piranha-treated nanosheets	
S5. Support synthesis	S17
S5.1 Silica support	S17
S5.2 Alumina flat support	S18
S5.3 Porous polymer (PBI) support	S19
S5.4 Alumina hollow fiber support	S19

Figures S1-S9	S21-S29
Tables S1-S16	S30-S46
Bibliography	S47-S49

S1. Complex chemical compounds

This section describes the method of synthesis of tetraethyl orthosilicate (TEOS), tetrapropylammonium hydroxide (TPAOH), polybenzimidazole (PBI), polyethylene glycol (PEG), dimethylacetamide (DMAc), polysulphone, n-methyl-2-pyrrolidone (NMP), and diquaternary ammonium surfactant (DQAS) from base chemicals, i.e., chemicals that exist in the GaBi 8.7® Pro database. The energy and the amount of raw material used in the synthesis of these compounds are given in **Table S1**.

S1.1. Tetraethyl orthosilicate

TEOS is simulated by the reaction between tetrachlorosilane and ethanol¹.

$$SiCl_4 + 4C_2H_5OH \rightarrow Si(OC_2H_5)_4 + 4HCl$$
 (1)

It has been considered a molar yield of 90 %. Energy required by this reaction has been calculated from bond energies with general formula:

$$\Delta H_r = \sum E_{bonds\ broken} - \sum E_{bonds\ formed}$$

Ethanol synthesis process is in-built in GaBi 8.7[®] Pro database and is described by the hydration of ethylene in a gas phase reactor with nitric acid as catalyst. SiCl₄ industrial synthesis is produced by reaction²:

$$Si + 2 Cl_2 \rightarrow SiCl_4$$
 (2)

It has been considered a molar yield of 90 %. Energies required by this reaction have been calculated from bond energies. Silicon and chlorine production processes are in-built in GaBi 8.7® Pro database.

S1.2. Tetrapropylammonium hydroxide

TPAOH is a quaternary amine and like most aliphatic amines its industrial synthesis involves reactions of ammonia with alkyl halides in polar media³ and then separation and purification:

$$NH_3 + 3C_3H_7Cl \rightarrow N(C_3H_7)_3 + 3HCl$$
 (3)

$$N(C_3H_7)_3 + C_3H_7Cl \rightarrow (C_3H_7)_4N^+Cl^-$$
 (4)

$$(C_3H_7)_4N^+Cl^- + NaOH \to (C_3H_7)_4N^+OH^- + NaCl$$
 (5)

By reaction (3) tertiary amine is obtained and by reaction (4) final quaternary amine is obtained. Per 1 gram of TPAOH produced, overall reaction is considered to be in 4 mL of acetonitrile/toluene media. 90 % of this solution is recovered by distillation. 0.1 mol of TPAOH is obtained per mol of NH₃. Finally, an anion exchange reaction is made (5). Energies required by these reactions have been calculated from bond energies. NH₃, NaOH, toluene and acetonitrile production processes are in-built in GaBi 8.7® Pro database. C₃H₇Cl has been considered to be produced by reaction (6) with 100 % molar yield:

$$C_3H_8 + HCl \rightarrow C_3H_7Cl + H_2 \tag{6}$$

Energy required by this reaction has been calculated from bond energies. Propane and hydrochloric acid production processes are in-built in GaBi 8.7® Pro database.

S1.3. Polybenzimidazole

It is a polymer obtained by polymerization reaction of 3,3'-diaminobenzidine and diphenyl isophthalate (reaction (7))⁴. For the calculation of the materials needed for the synthesis of 1 g of PBI it has been taken an average molecular weight of PBI = 32500 g/mol^5 .

$$NH_{2}$$
 NH_{2}
 N

If polymerization reaction yield is considered to be 100 %, it'll be necessary $4.83*10^{-4}$ mol of 3,3'-diaminobenzidine and of diphenyl isophthalate. For the energy requirements calculation, reactions take place on a reactor with a heat transfer coefficient of 120 kcal/h °C m² and exchange area of $1*10^{-6}$ m² (it's assumed a ratio 1 m³ : 1 m² between volume and transfer area).

S1.3.1. 3,3'-diaminobenzidine

3,3'-diaminobenzidine is obtained by the reaction of 3,3'-dichlorobenzidine and ammonia at high pressures and temperatures and with copper catalyst⁶ (reaction (8)). It's assumed a molar yield of 90 % and 2 %_w of the catalyst. 100 % of the copper is recovered by electrolysis. Energy required for electrolysis has been calculated taking into account copper reduction potential. For the calculation of the energy required for this synthesis, reactions take place on a reactor with the same characteristics as before.

$$NH_{2}$$
 $+ 2 NH_{3}$ $\xrightarrow{T > 300 °C}$ NH_{2} $+ 2 HC$ $+ 2 HC$

3,3'-dichlorobenzidine is obtained by reaction of 2-nitrochlorobenzene with zinc dust and NaOH (reaction (9)). This reaction is made in organic media like toluene media and is exothermic⁷. It's assumed a molar yield of 90 %. 1/3 of the zinc used is considered to be produced from raw materials and the product sodium zincate is electrolyzed to be reused as Zn. Energy for electrolysis has been calculated taking into account Zn reduction potential. Zn production processes is in-built in GaBi 8.7[®] Pro database.

2-nitrochlorobenzene is produced by reaction of chlorobenzene and nitric acid in presence of sulfuric acid (reaction (10)) ⁸. It's assumed a molar yield of 90 % and 2 %_w of the catalyst. For the calculation of the energy required for the synthesis, bonds energies are used. Nitric and sulfuric acids production processes are in-built in GaBi 8.7[®] Pro database

$$\begin{array}{c|c} CI & NO_2 \\ + HNO_3 & + 1/2 H_2O + 1/4 O_2 \end{array}$$
2-chlorobenzene 2-nitrochlorobenzene (10)

Finally, chlorobenzene is produced by chlorination of benzene in presence of FeCl₃⁹. It's assumed a molar yield of 90 % and 2 %_w of the catalyst. FeCl₃ is industrially produced by reaction of dry chlorine with scrap iron at 500-700 °C. To prevent formation of iron (II) chloride, a 20 % excess of chlorine is used. The reaction is made on industrial furnaces with 340 L of capacity and with an electric source of 400 kW. The reaction takes place during 4 hours¹⁰. Magnetite mineral is used as iron source and 60 % of the volume of the furnace is occupied by magnetite. Iron ore extract

process is not in GaBi 8.7[®] Pro database but iron ore flux is with its respective associated impact to the Resource Depletion Mineral environmental indicator. Benzene production process is in-built in GaBi 8.7[®] Pro database

S1.3.2. Diphenyl isophthalate

Diphenyl isophthalate is obtained by the reaction of phthalic anhydride and toluene in presence of H_2SO_4 (reaction (11))¹¹. It's assumed a molar yield of 90 % and 2 %_w of the catalyst. For the calculation of the energy required for the synthesis, bonds energies are used.

Phthalic anhydride is obtained by o-xylene oxidation with V₂O₅ as catalyst at 320-400 °C¹¹ with 70 % of selectivity to this product (reaction (12)). Vanadium (V) oxide is produced from vanadium slags derived from the ores. Vanadium ore is pre-reduced at 1000 °C. A further reduction is then performed in an electric arc furnace to obtain a pig iron which contains 1.4 % V₂O₅. The pig iron is oxidized and the slag produced. Then the slag is treated with NaCl and roasted with oxidation at 700-850 °C. The roasted product is leached with water and ammonium polyvanadate is precipitated from the alkaline sodium vanadate solution by adding sulfuric or chloric acid at high temperatures. Finally, a roast is done¹². Ovens and furnaces are considered of 400 kW of electric power and 4 hours of reaction. 350 L of oven and furnace volume are considered. NaCl and sulfuric acid addition volumes are 10 % in weight of the vanadium oxide produced. Magnetite mineral is considered the source of Vanadium ore (0.95 % of vanadium)¹³ with a density of 5.046 kg/L. Finally, o-xylene is produced by naphtha cracking¹⁴. Naphtha and NaCl production processes are in-built in GaBi 8.7® Pro database. Vanadium ore extract process is not in GaBi 8.7® Pro database.

but vanadium ore flux is with its respective associated impact to the Resource Depletion Mineral environmental indicator. It's assumed a molar yield of 90 % and 2 ‰ of the catalyst. For the calculation of the energy required for the synthesis, reactions take place on a reactor with the same characteristics as before.

$$\begin{array}{c}
\text{CH}_{3} \\
\text{CH}_{3}
\end{array}$$

$$\begin{array}{c}
\text{CH}_{3} \\
\text{+ 3 O}_{2}
\end{array}$$

$$\begin{array}{c}
\text{V}_{2}\text{O}_{5} \\
\text{320-400 °C}
\end{array}$$

$$\begin{array}{c}
\text{O} \\
\text{O}
\end{array}$$

$$\begin{array}{c}
\text{O} \\
\text{+ 3 H}_{2}\text{O}
\end{array}$$

$$\begin{array}{c}
\text{O} \\
\text{Phthalic anhydride}
\end{array}$$

S1.4. Dimethylacetamide

Dimethylacetamide is prepared by the reaction of dimethylamine with acetone at 325 °C and pressure 6.5 MPa with a yield of 50 %¹⁵. For the calculation of the energy required for the synthesis, reactions take place on a reactor with the same characteristics as before. Acetone production process is in-built in GaBi 8.7[®] Pro database, but not dimethylamine. Dimethylamine is industrially produced by catalytic reaction of methanol and ammonia at elevated temperatures and high pressures (reaction (13))¹⁶.

$$2CH_3OH + NH_3 \xrightarrow{Mordenite\ catalyst} (CH_3)_2NH + 2H_2O$$
 (13)

Methylamines selectivities (wt.%) from this catalyst are reported to be 33.3% monomethyl amine, 63% dimethyl amine, and 3.7% tri-methyl amine at 90% methanol conversion, and 1.9 molar ratio ammonia: methanol. It's assumed 2 %w of the catalyst. For the calculation of the energy required for the synthesis, bonds energies are used. Methanol production process is not in-built in GaBi 8.7® Pro database and has been simulated by reaction of carbon monoxide and hydrogen. CO and H₂ production processes are in-built in GaBi 8.7® Pro database. Mordenite production process is

not in-built in GaBi 8.7® Pro database and its production process has been considered to be as silicalite-1 seeds production process.

S1.5. Polyethylene Glycol

Polyethylene glycol is obtained by polymerization of ethylene glycol and ethylene oxide (reaction (14))¹⁷:

$$HOCH_2CH_2OH + n(CH_2CH_2O) \xrightarrow{NaOH} OH(CH_2CH_2O)_{n+1}H$$
(14)

It has been considered n=80, 100% of efficiency of polymerization reaction, that takes place on 4 mL of EtOH as dissolvent per gram of product, and 2 %_w of limiting reactive to calculate the use of catalyst. For the calculation of the energy required for the synthesis, reactions take place on a reactor with the characteristics as before. Ethylene glycol production process is in-built in GaBi 8.7[®] Pro database but Ethylene oxide not.

Ethylene oxide is industrially produced by direct oxidation of ethylene with silver catalyst¹⁸ with a maximum conversion of 85.7 % and exothermic enthalpy of 105 kJ/mol (reaction (15)). Silver has been recovered by electrolysis and the energy used has been calculated with its reduction potential. Ethylene and oxygen production processes are in-built in GaBi 8.7® Pro database.

$$7CH_2 = CH_2 + 6O_2 \xrightarrow{Ag} 6(CH_2CH_2)O + 2CO_2 + 2H_2O$$
 (15)

S1.6. Polysulfone

Polysulfone is prepared by a polycondensation reaction of the sodium salt of an aromatic diphenol and bis(4-chlorophenyl)sulfone and its molecular weight is considered to be 19000 g/mol (reaction (16))¹⁹. The polymerization is carried out at 130–160 °C under inert conditions in a polar solvent. For the calculation of the energy required for the synthesis, reactions take place on a reactor with the characteristics as before.

n
$$CI \longrightarrow SO_2 \longrightarrow CI + n NaO \longrightarrow NaO \longrightarrow$$
bis(4-chlorophenyl)sulfone (16)
$$\longrightarrow SO_2 \longrightarrow O \longrightarrow P + 2 n HCI$$

The sodium salt of an aromatic diphenol has been simulated by the direct reaction of sodium hydroxide and phenol. Phenol and sodium hydroxide production processes are in-built in GaBi 8.7® Pro database. Bis(4-chlorophenyl)sulfone has been simulated by direct reaction of chlorobenzene and sulphuric acid. Chlorobenzene production process has been simulated before (Section 1.3.1).

S1.7. N-methyl-2-pyrrolidone

NMP (N-methyl-2-pyrrolidone) is industrially produced by reaction $(17)^{20}$ but it is considered to be produced by a simplified reaction of methylamine and butanediol because butyrolacytone is directly produced by dehydration of butanediol (reaction $(18)^{21}$. Methylamine has been simulated as before dimethylamine with methanol and amine with mordenite catalyst. Butanediol production process is in-built in GaBi 8.7° Pro database. For the calculation of the energy required for the synthesis, bonds energies are used.

$$+ NH_2 - CH_3 \longrightarrow + H_2O$$
butyrolactone
$$CH_3$$

$$N-Methyl-2-pyrrolidone$$
(17)

S1.8. Surfactant C₂₂₋₆₋₆(OH)₂

It is obtained by alkylation of N,N,N',N'-tetramethyl-1,6-hexanediamine $(CH_3)_2N(CH_2)_6N(CH_3)_2$ with 1-bromodocosane $CH_3(CH_2)_2$ Br and 1-bromohexane $CH_3(CH_2)_5$ Br²²:

$$(CH_{3})_{2}N(CH_{2})_{6}N(CH_{3})_{2} + CH_{3}(CH_{2})_{21}Br \rightarrow (CH_{3})_{2}N(CH_{2})_{6}N(CH_{3})(CH_{2})_{22}Br + H_{2}$$
(19)

$$(CH_{3})_{2}N(CH_{2})_{6}N(CH_{3})(CH_{2})_{22}Br + CH_{3}(CH_{2})_{5}Br \rightarrow Br(CH_{2})_{6}(CH_{3})N(CH_{2})_{6}N(CH_{3})(CH_{2})_{22}Br + H_{2}$$
(20)

The impact of 1 mol of surfactant $C_{22-6-6}(OH)_2$ is considered equivalent to the combined impacts of 1 mol of hexanomethylenediamine, 1 mol of C22 alkene, 1 mol of C13 alkene and 4 moles of C1 alkene. The four compounds are in-built in GaBi $8.7^{\$}$ Pro database.

S2. Seed layer synthesis

S2.1 Conventional seed layer

The material and energy flows for conventional seed layer method are calculated using the procedure described in²³. The seeds are obtained by stirring TEOS and TPAOH in water (molar ratio of 6 TEOS: 0.9 TPAOH: 620 H₂O). Assuming that 0.45 mg of silicalite-1 seeds are supported, the corresponding amounts of TEOS, TPAOH and water are calculated for the synthesis (Figure S1) considering their corresponding molar mass and that for one mol of TEOS, one mol of SiO₂ is obtained. 90 % of the water used is considered to be reused. A polymeric solution of polyacrylic acid and ethylene glycol (mass ratio of 5 H₂O: 5 polyacrylic acid: 2 ethylene glycol) is then spin coated onto the support. This step is repeated twice to ensure entire surface coverage by polymeric film. Polymeric suspension of 1 µm thickness is assumed for the calculation of material required. Considering support area of 3.8e-4 m², the polymeric thickness, and mass ratio of polymeric solution it's possible to calculate corresponding amounts of polyacrilic acid, water and ethylenglycol (**Figure S1**). Finally, the support is rubbed with silicalite seeds followed by rubbing with 1 µm spherical silica particles. Considering a monolayer of silica particles, that these particles are spheres of 1 µm, and silica density as 2650 kg/m³, it's possible to calculate silica mass required (Figure S1). All the mass inputs calculated for conventional seed layer synthesis at laboratory scale and complied on Figure S1 have been multiplied by scaling factor (1000 m²/0.00038 m²) to take into account industrial scale synthesis. These amounts at industrial scale have been used for energy calculations. For the purposes of comparison, support is not considered in energy inputs calculations. Three thermal processes have been considered (Figure S1). The first one is the crystallization of TEOS and TPAOH in water solution at 150°C during 12 h. First, energy required to raise the temperature to 150°C from 25 °C has been calculated for TEOS, TPAOH and water using specific heats and masses of each component at industrial scale (7.66 kWh). Second, heat of vaporization of water is calculated (32.04 kWh). Finally, energy to keep temperature at 150°C during 12 h has been calculated multiplying the heat used to raise temperature by a thermal insulator factor of 0.1 and by time (9.19 kWh). Total energy required to crystallization is 48.88 kWh. The same procedure has been used to calculate energy for the thermal treatment at 70 °C during 1 h of polymeric solution. In this case polyacrilic acid, water, and ethylenglycol have been thermally treated and final energy is 35.24 kWh. Finally, energy for the calcination of silica, TPAOH and TEOS have been calculated following same procedure and considering TPAOH is going to be sublimated (2.13 kWh). The total energy requirements for silicalite-1 conventional seeds synthesis at industrial scale are 86.25 kWh.

S2.2 Multi-lamellar nanosheet seed layer

The material and energy flows for nanosheet seed layer method are calculated using the procedure described in²⁴. A gel molar composition of 100 TEOS: 15 DQAS (diquaternary ammonium surfactant): 4000 H₂O: 400 Ethanol was considered after crystallization at 150 °C for 5 days for the nanosheets synthesis. Amounts of each compound have been calculated using the amount of seeds over the support (0.06 mg), gel molar composition, and considering that one mol of TEOS is equivalent to one mol of ML-MFI (**Figure S2**). 90 % of water and ethanol are reused. The nanosheets were exfoliated by mixing them with polystyrene followed by dissolution of the zeolite-polymer nanocomposite in toluene in the mass ratio of 1.25 polystyrene: 0.05 MFI-zeolite: 87.5 toluene. 90 % of the toluene is recovered by distillation. The amounts of each compound required are shown in **Figure S2**. The suspension, obtained by dispersion and purification, was vacuum-filter coated on the support and calcined at 540 °C for 6 h to obtain the seed layer. All the mass inputs calculated for ML-MFI seeds layer synthesis at laboratory scale and complied on

Figure S2 have been multiplied by scaling factor to take into account industrial scale synthesis. Regarding energy inputs, energy required for crystallization at 150 °C during 5 days has been calculated following procedure explained in previous section considering also vaporization of ethanol (1.13 kWh). Energy required for calcination has been calculated considering sublimation of TEOS too (0.31 kWh). Finally, energy for toluene distillation has been calculated considering specific heats, and temperature and vaporization heats, and toluene mass distillated (281 kg) (39.46 kWh). The total energy requirements for the ML-MFI seeds layer synthesis at industrial scale are 40.9 kWh.

S3. Secondary growth method

S3.1 Solvent-based sol-gel method

The material and energy flows for solvent-based sol-gel secondary growth method are calculated using the procedure described in²⁴. The seeded calcined support was placed in a solution of 60 TEOS: 9 TPAOH: 8100 H20: 240 Ethanol (molar composition) aged at 90 °C for 6 h. It has been considered that 90 % of TEOS and TPAOH are reused and also that consumption during secondary growth of these compounds is 20 %, and of water and EtOH is 10%. The amounts of each compound used at laboratory scale are compiled in **Figure S3**. The solution, containing the support was further heated for 4.5 h at 90 °C. As the secondary growth fills the crack without much change in the thickness, it is considered that only TPAOH is consumed in the growth. 10 ml of the solution (with composition stated above) was used to calculate the amount of materials. The solid was then calcined at 480 °C for 4 h to remove the SDA and obtain a porous membrane. All the amounts calculated at laboratory scale and showed in **Figure S3** have been multiplied by industrial scaling factor to calculate amounts used at industrial scale. These amounts have been used to calculate energy requirements following procedure explained above and using also specific heats of each

component and heat of vaporization of water and ethanol, for the two thermal treatments at 90 °C (1755.7 kWh and 1727.3 kWh, respectively). For the calcination at 480 °C 4 h, only TPAOH and TEOS has been considered with their specific heats, and heat of sublimation of TPAOH (137.81 kWh). The total energy requirements for the solvent-based sol-gel method at industrial scale are 3620.71 kWh.

S3.2 Gel-less (gel-free) method

The material and energy flows for gel-less (gel-free) secondary growth are calculated using the procedure described in²⁵. The calcined support was impregnated with a solution of 0.025 M solution of TPAOH followed by heating at 90 °C for 48 h. 1 ml of the solution is considered for coating on the seeded support to calculate the amounts of materials used (**Figure S4**). All the amounts calculated at laboratory scale and showed in **Figure S4** have been multiplied by scaling factors to calculate amounts used at industrial scale. Regarding energy calculation specific heats of water and TPAOH and heat of vaporization of water are used (2793.15 kWh).

S4. Piranha-treated nanosheets

The material and energy flows for piranha-treated open-pore membrane synthesis method are calculated using the procedure described in²⁶. The as-synthesized ML-MFI seeds (without exfoliation), similar to those obtained for nanosheet seed method, were treated with Piranha solution four times. The aim of this step is twofold: (i) exfoliation of the ML-MFI, and (ii) removal of SDA. For every 1 g of ML-MFI nanosheets, 20 ml of H₂O₂ and 60 ml of H₂SO₄ (30 wt. % in water) are required. These open pore nanosheets were filter coated on the support to obtain the membrane. 90% of the acid solution is recovered by distillation. A 500 nm thickness coating of MFI nanosheets is assumed. Amounts of each compound are showed in **Figure S5**. Energy for crystallization and sintering has been neglected (**Section S2.2.**) Regarding energy calculation only

energy used during distillation of acid solution is considered. It has been calculated considering masses used and specific heats, and temperatures and heats of vaporization of each component. As it has been said in the main text, since membranes are prepared without any secondary growth, the impact of this method is compared to the combined impact of the seed layer synthesis and secondary growth. For this reason in this section, amounts of compounds (TPAOH, DQAS, water and ethanol) to prepare 500 nm thickness coating of MFI nanosheets are considered (**Figure S6**).

S5. Support synthesis

S5.1 Silica support

The material and energy flows for synthesis of silica support are calculated using the procedure described in²⁵. 1.7 g of quartz wool is pressed and mixed with 12 drops of 0.5 % (w/w) solution of poly(vinyl alcohol) (PVA) in water. The mixture was then dried at 70 °C for 12 h followed by sintering at 1230 °C for 3 h. The support was then polished and coated three times with 500 nm (3 times) and with 50 nm (1 time) silica nanoparticles. After each coating, the support was dried at 70 °C for 4 h followed by thermal treatment at 1,100 °C for 3 h (500 nm particles) or 400 °C for 4 h (50 nm particles).

As for the synthesis of the silica nanoparticles, tetraethyl orthosilicate (TEOS), ammonia 30%_w, ethanol and water (molar ratio of 1:11.8:50:52.3 for the 500 nm particles and 1:0.43:53.6:58.6 for the 50 nm particles) were stirred. The nanoparticles were collected by centrifugation, washed with ethanol followed by calcination at 1000 °C for 3 h (for the 500 nm particles) or at 400 °C for 3 h (for the 50 nm particles). A 10 µm thick layer is considered for the 500 nm particles while a 200 nm thick layer is considered for 50 nm particles in order to calculate the amounts of materials used. For the calculations of each amount it has been considered that silica particles are spheres and

silica density 2650 kg/m³. 500 nm particles weigh is 6.71 mg and 50 nm is 0.134 mg. The amounts used as well as the overall process is shown in **Figure S7**.

Regarding energy calculations it has been followed the procedure explained above. For drying of the support, specific heat of quartz and water, and heat of vaporization of water, and industrial scale amounts of each compound have been considered (1252.10 kWh). For the sintering at 1230°C only quartz specific heat has been considered (1417.1 kWh). Energy for 500 nm and 50 nm silica synthesis has been calculated considering TPAOH specific heat (37.7 and 0.3 kWh, respectively). For drying and sintering of support coated with 500 nm silica particles quartz and silica specific heats, amounts of quartz and 500 nm particles at industrial scale have been considered, and the fact that the process is repeated three times (176.6 and 3953.7 kWh, respectively). For drying and sintering of support coated with 50 nm silica particles quartz and silica specific heats and amounts of quartz and 50 nm particles at industrial scale have been considered (58.9 and 490.8 kWh, respectively). The total energy requirements for silica support preparation method at industrial scale are 7386.2 kWh.

S5.2 Alumina flat support

The material and energy flows for synthesis of alumina support are calculated using the procedure described in^{27,28}. Alumina discs were prepared by pressing alumina powder and sintering at 1160 °C for 6 h. A support thickness of 3 mm and a porosity of 0.3 have been considered. The total amount of alumina calculated for the laboratory scale preparation is 3.15 g. For energy calculations, specific heat and amount at industrial of alumina have been used (3671.16 kWh). Alumina manufacture process is not in-built in GaBi 8.7® Pro database, so it has been simulated following manufacture process described in²⁹.

S5.3 Porous polymer (PBI) support

The material and energy flows for synthesis of PBI polymer support are calculated using the procedure described in²⁶. A polymer solution of polybenzimidazole (PBI), dimethyl acetamide (DMAC) and polyethylene glycol (PEG) in mass ratio of 15:85:5 was stirred overnight at 75 °C followed by cooling at room temperature for 1 day. The solution was casted on a porous stainless steel mesh disc (500 µm thickness) followed by transferring in a water bath set at 50 °C. The water was exchanged out of the membrane in methanol and hexane bath followed by drying under air at 300 °C for 3 h to obtain the support. **Figure S8** shows amounts of each compound used for the laboratory scale support synthesis. It has to be noted that stainless steel mesh disc it has not been considered. Regarding energy calculation, amounts of DMAc, PBI and PEG at industrial scale and their specific heats have been considered for thermal treatments at 70 °C and 300 °C (39.41 and 139.2 kWh, respectively). For distillation of DMAc, amount at industrial scale, specific heat and heat of vaporization have been used (172.3 kWh). The total energy requirements for PBI support preparation method at industrial scale are 342.95 kWh

S5.4 Alumina hollow fiber support

The material and energy flows for synthesis of alumina hollow fiber support are calculated using the procedure described in³⁰. Hollow fiber supports of 1.0 mm inner diameter and 1.6 mm outer diameter were prepared. A well-mixed solution of the ceramic/polymer/solvent/additive (alumina/polyethersulfone/n-methyl-2-pyrrolidone/polyvinyl-pyrrolidone) in a 38:8.8:52.7:0.5 mass ratio was stirred and degassed. For the calculations of the amounts of each component, volume of the support has been calculated using a porosity of 0.5 and density of 2 g/cm³. Also a length of 7.33 cm (resulting in an equivalent surface area similar to the other supports considered) was used to calculate the amounts of materials required. The same mass of water than n-methyl-

2-pyrrolidone is added. The amounts of each material needed for the alumina hollow-fiber support manufacture at laboratory scale are shown in **Figure S9**. The hollow fiber precursor was obtained by phase inversion, being dried in oven at 60 °C for 6 h, heated in electric furnace at 500 °C for 2 h and 1000 °C for 2 h followed by calcination at 1,500 °C for 4 h. Regarding drying step, energy used was calculated using amounts and specific heat of the five components, and also heat of vaporization of water (63.73 kWh). For polymer removal step, amounts and specific heats of alumina, polyethersulfone, n-methyl-2-pyrrolidone, polyvinyl-pyrrolidone are considered, and also heat of sublimation of polyethersulfone (21.79 kWh). For the two final thermal processes, alumina and PVP amounts and specific heats are considered (30.68 and 64.97 kWh, respectively).

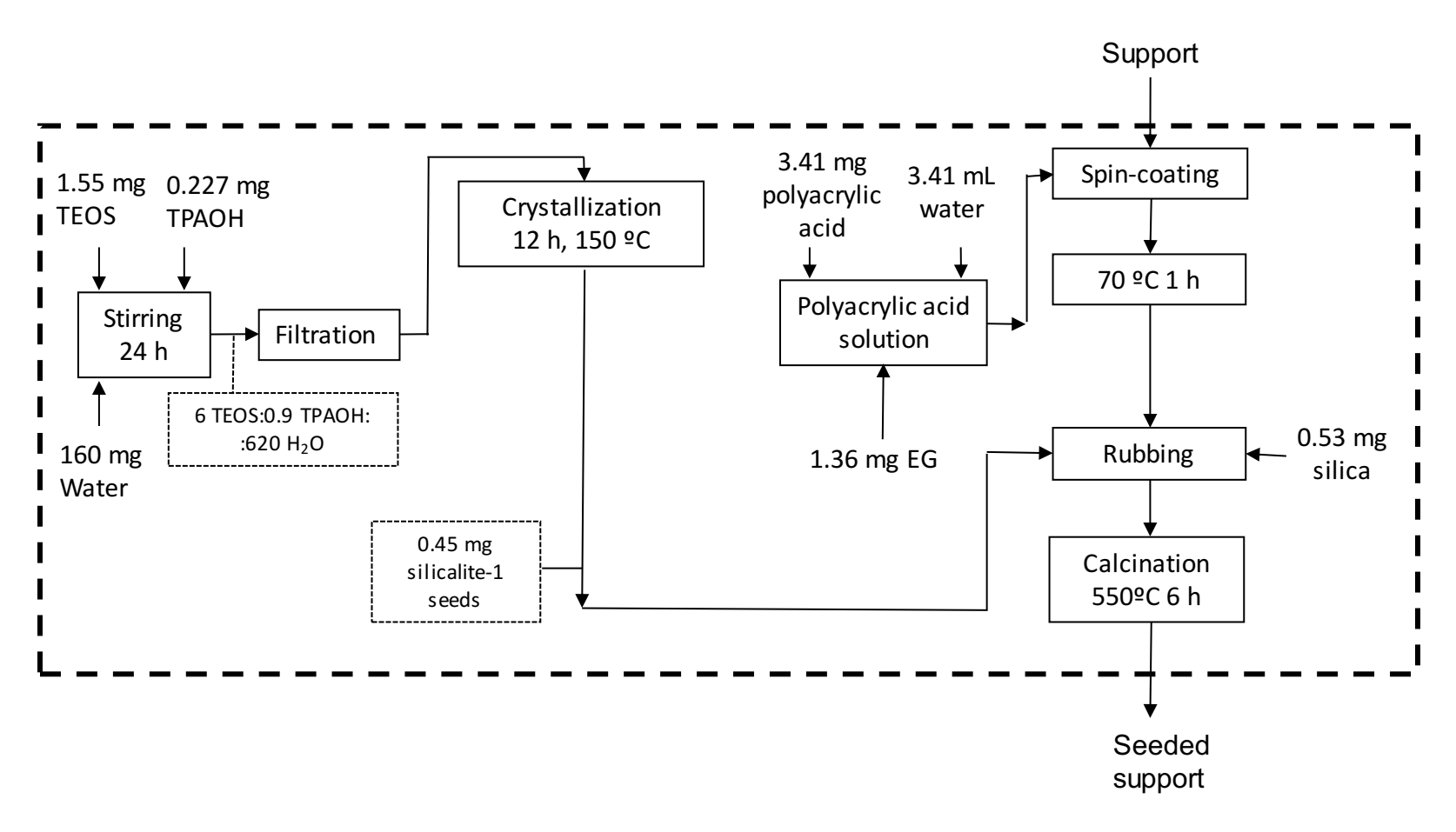


Figure S1 – Conventional seeds layer synthesis process at laboratory scale and system boundaries (dotted line) of the LCA study.

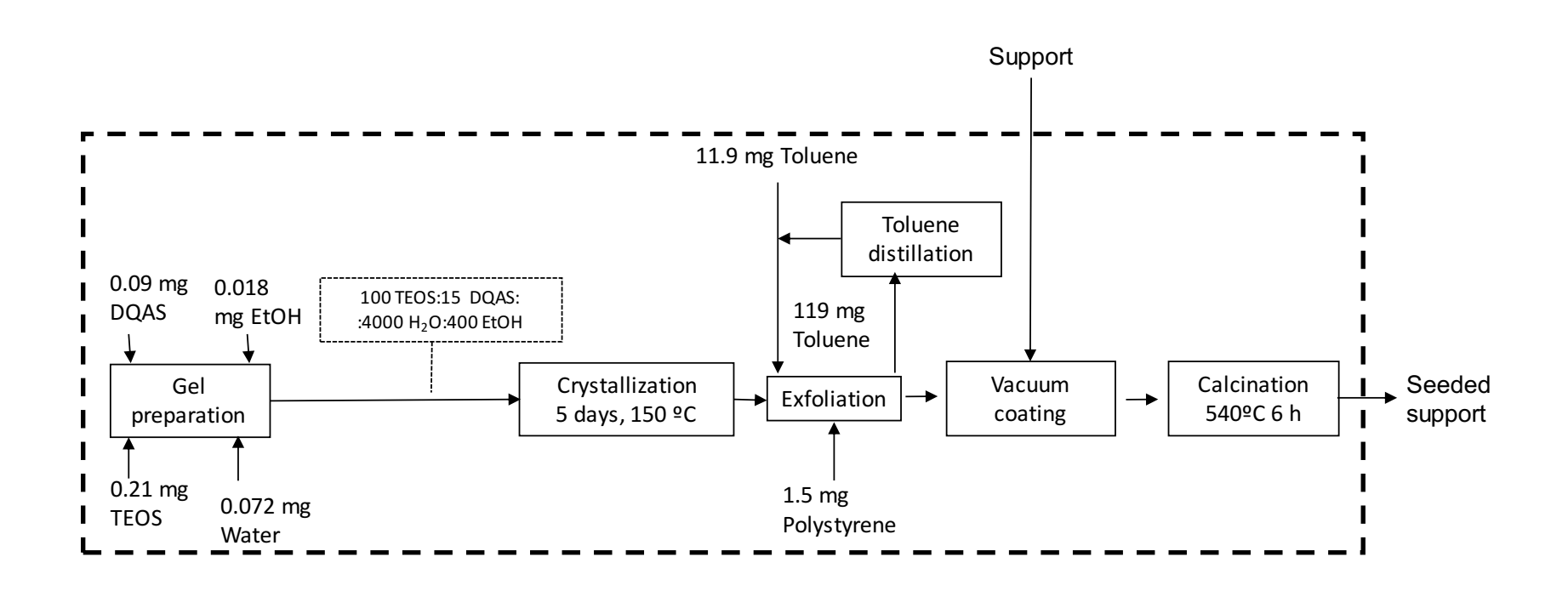


Figure S2 – ML-MFI seeds layer synthesis process at laboratory scale and system boundaries (dotted line) of the LCA study.

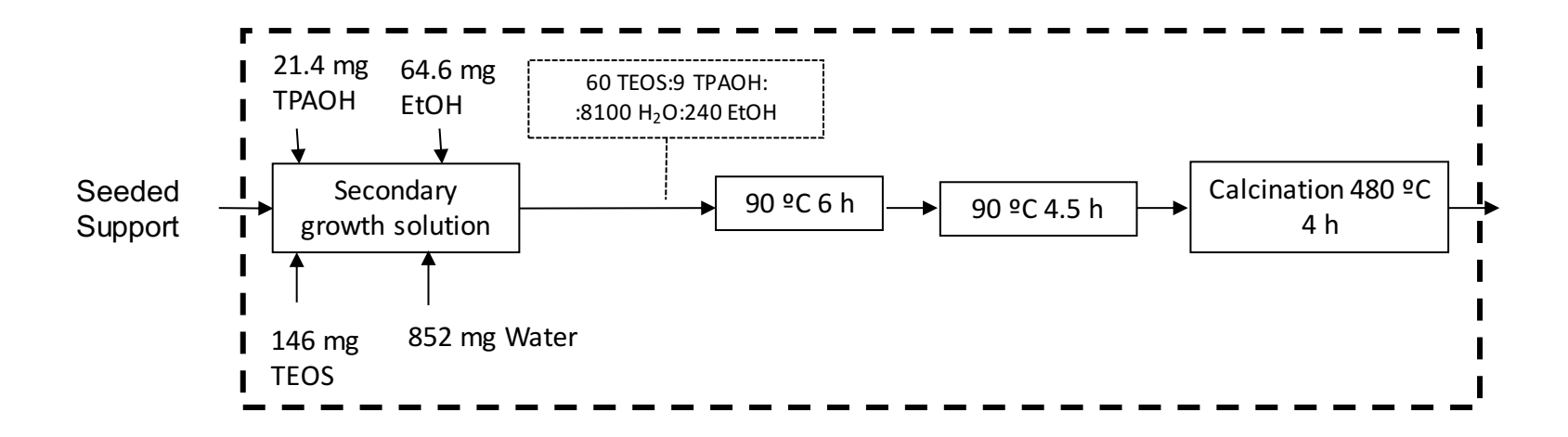


Figure S3 – Solvent-based sol-gel process for secondary growth at laboratory scale and system boundaries (dotted line) of the LCA study.

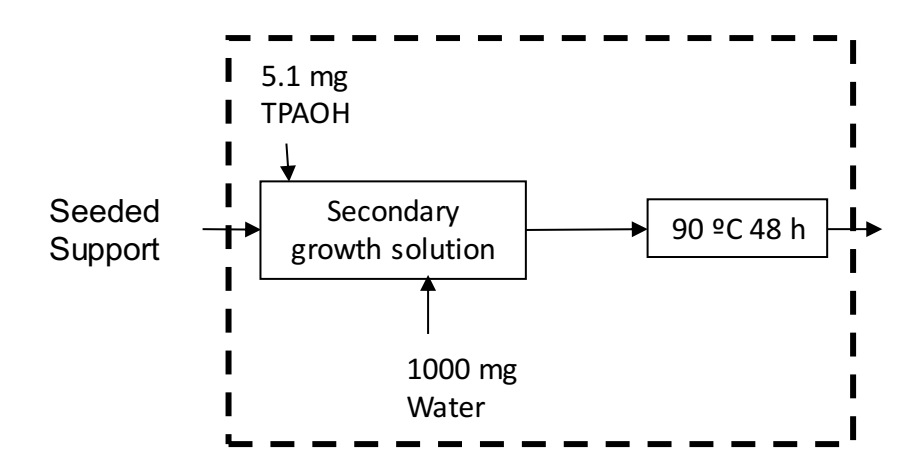


Figure S4 – Gel-less (gel-free) process for secondary growth at laboratory scale and system boundaries (dotted line) of the LCA study.

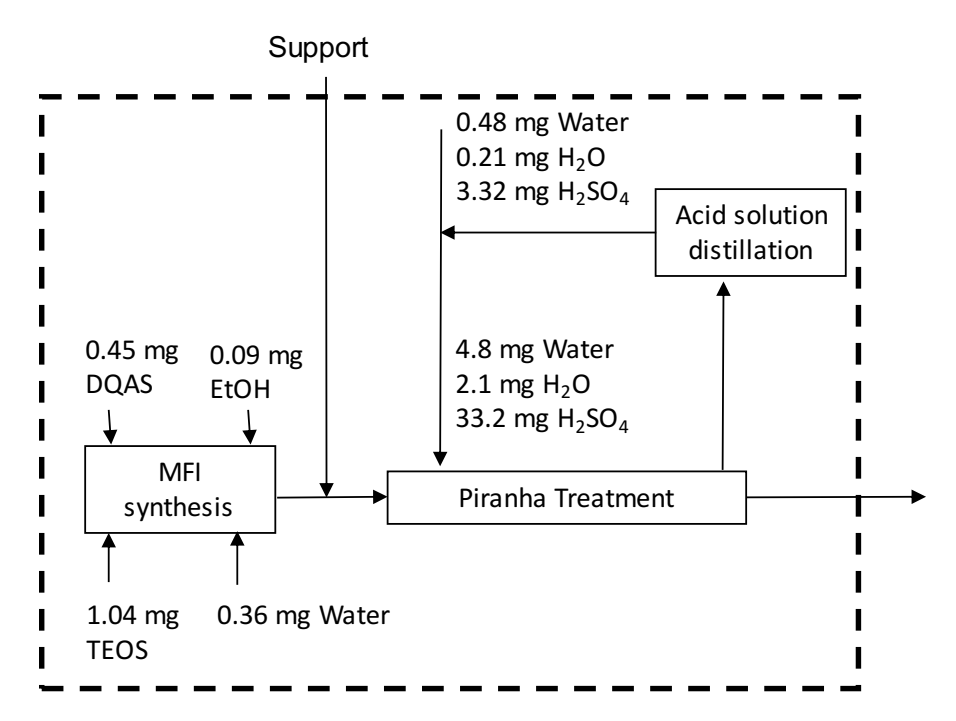


Figure S5 – Piranha treatment process and ML-MFI synthesis at laboratory scale and system boundaries (dotted line) of the LCA study.

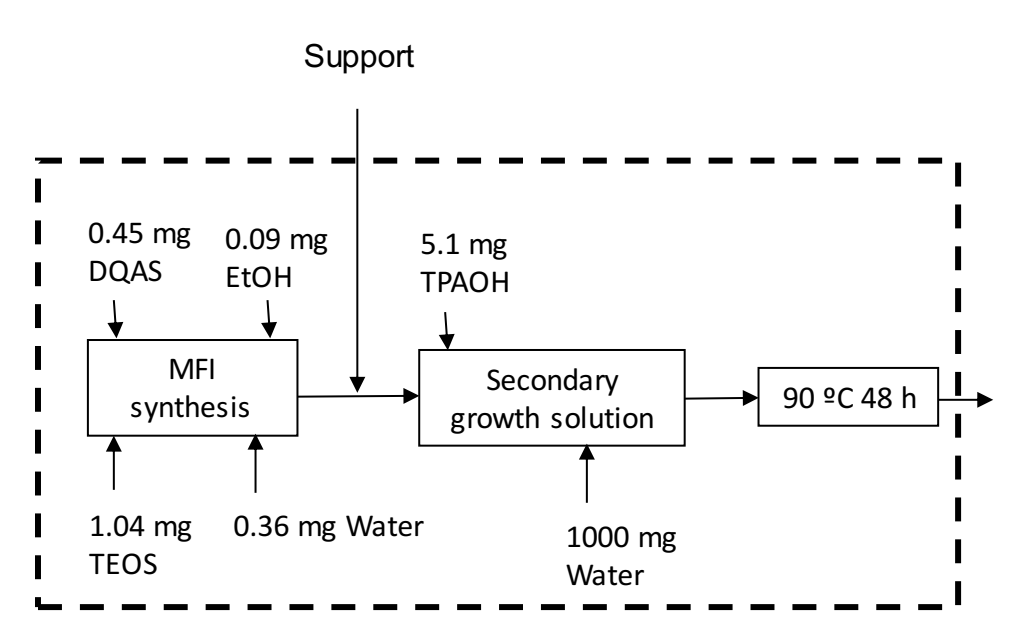


Figure S6 – Gel-free process and ML-MFI synthesis at laboratory scale and system boundaries (dotted line) of the LCA study.

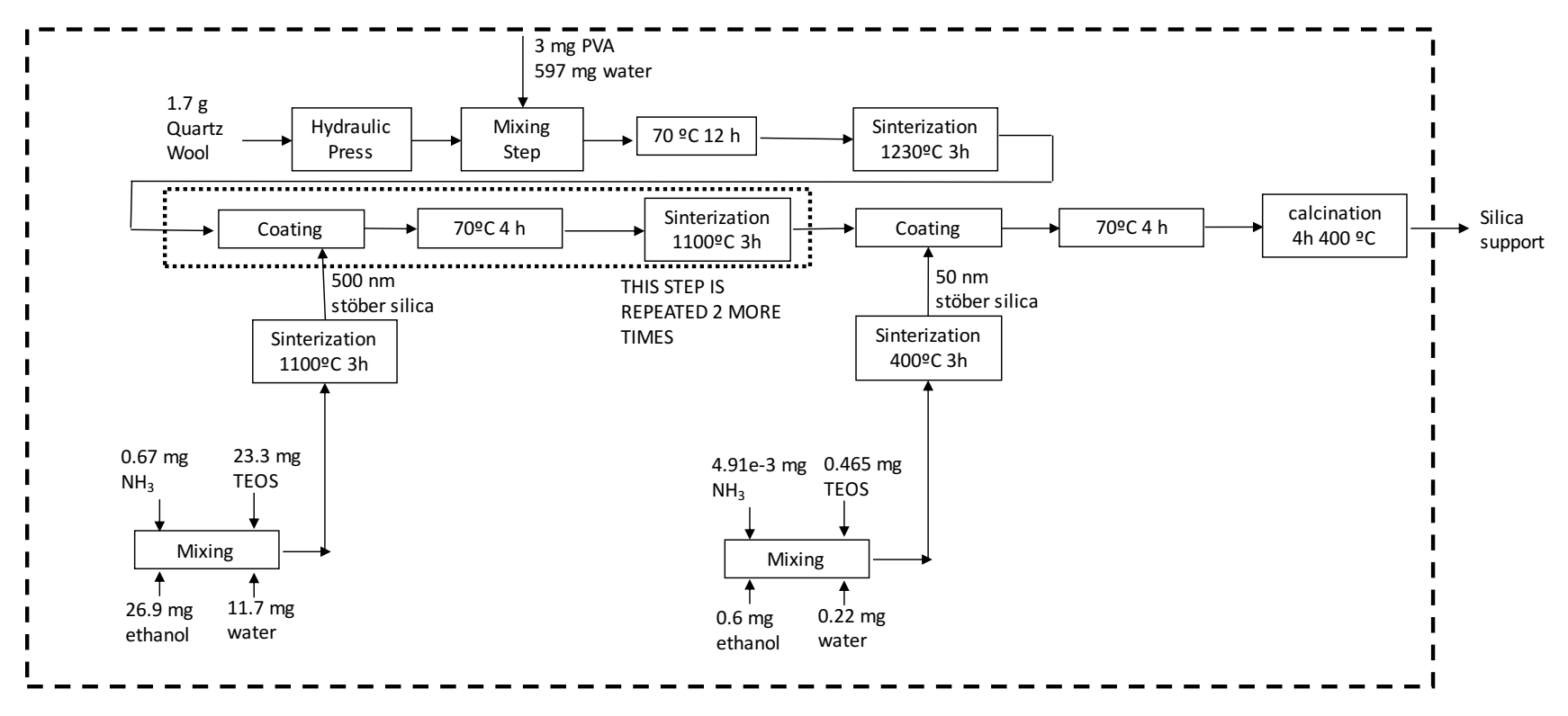


Figure S7 – Quartz support preparation process at laboratory scale and system boundaries (dotted line) of the LCA study.

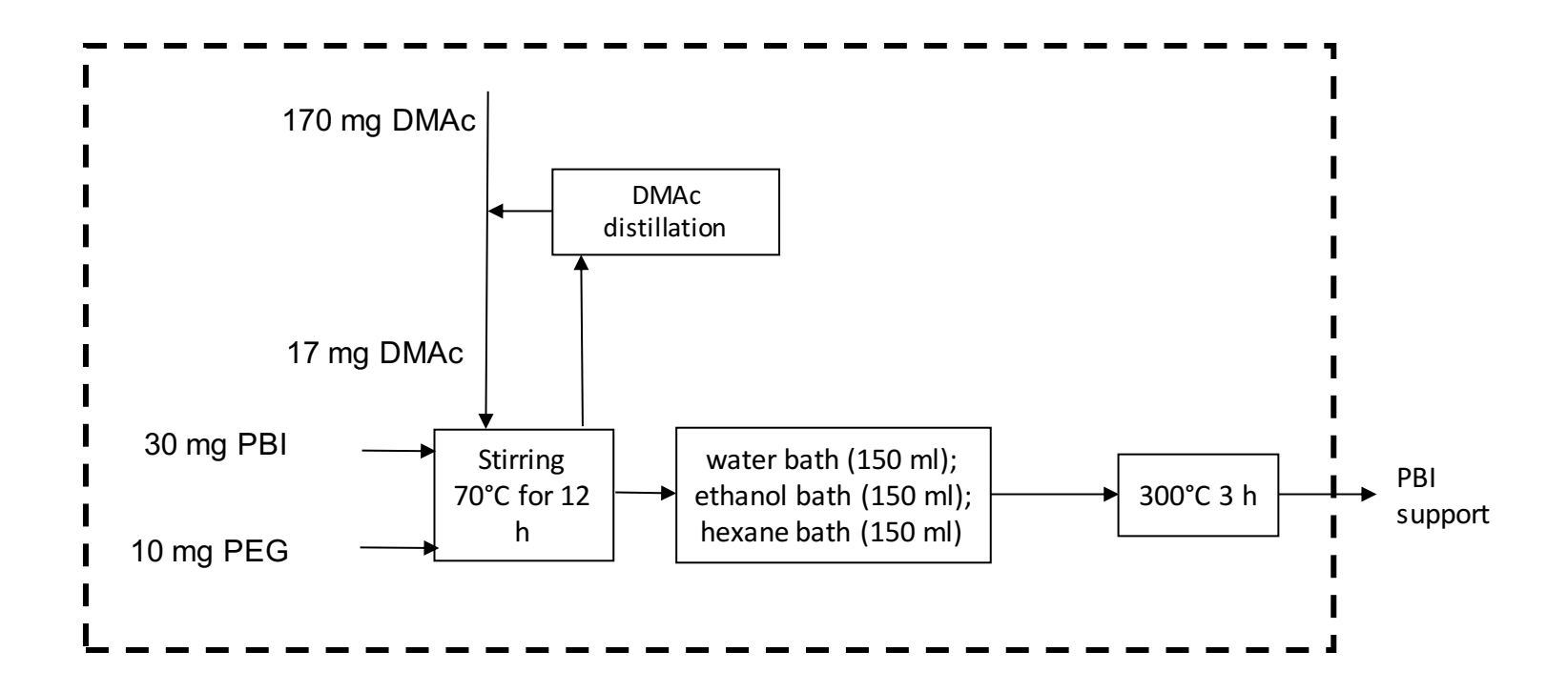


Figure S8 – PBI support preparation process at laboratory scale and system boundaries (dotted line) of the LCA study.

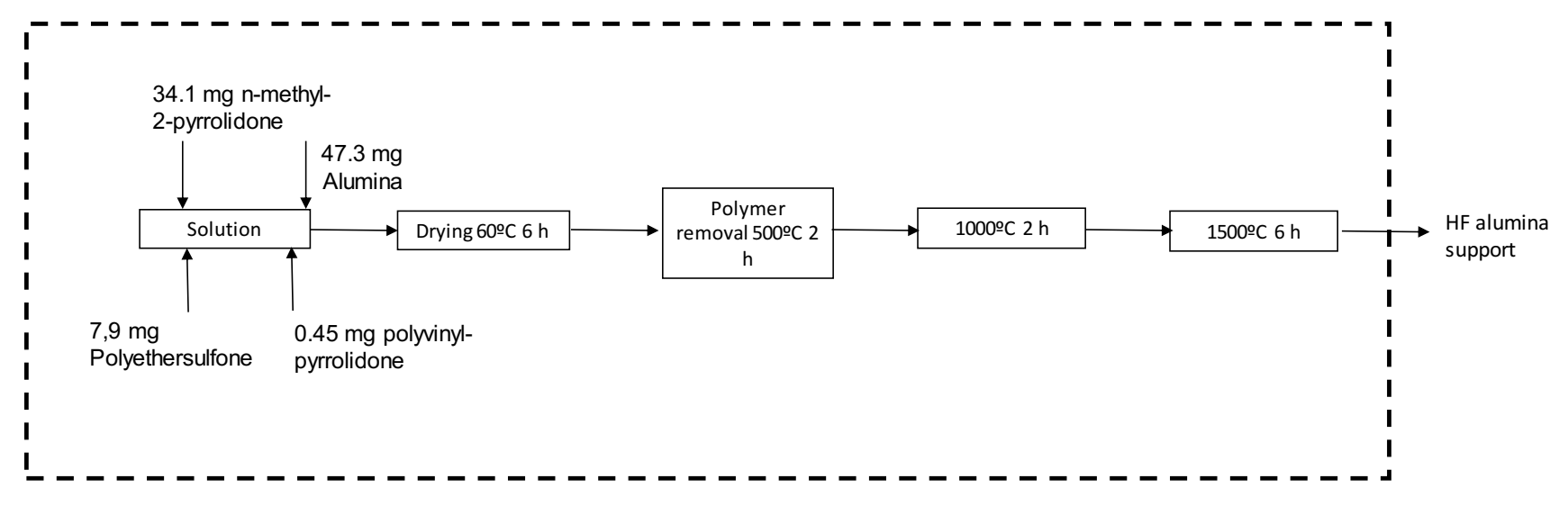


Figure S9 – Alumina hollow-fiber support preparation process at laboratory scale and system boundaries (dotted line) of the LCA study.

Table S1. Material (g) and thermal energy (kJ) input for synthesis of 1 g of the compounds indicated

Compound	PBI	DMAc	ТРАОН	TEOS	PEG	Polysulfone	NMP	DQAS
Thermal Energy	3.58E+01	1.03E+00	1.29E+01	-	-	-	-	-
Toluene	7.13E-03	-	1.80E-01	-	-	-	-	-
Copper	1.53E-02	-	-	-	-	-	-	-
Ammonia	1.20E-01	-	8.40E-01	-	-	-	2.00E-01	-
Sodium hydroxide	1.60E+00	-	2.00E+00	-	3.46E-04	9.00E-02	-	-
Nitric acid	5.60E-01	-	-	-	-	-	-	-
Sulfuric acid	5.07E-02	-	-	-	-	2.20E-01	-	-
Vanadium (V) oxide	1.18E-02	-	-	-	-	-	-	-
Benzene	7.30E-01	-	-	-	-	3.50E-01	-	-
Chlorine	6.70E-01	-	-	8.40E-01	-	3.20E-01	-	-
Xylene	5.30E-01	-	-	-	-	-	-	-
Oxygen	5.00E-02	-	-	-	8.40E-01	-	-	-
Iron (III) chloride	2.20E-02	-	-	-	-	1.20E-04	-	-
Zinc	1.27E+00	-	-	-	-	-	-	-
Electricity electrolysis/distillation	1.40E+01	-	-	-	2.92E+00	-	-	-
Acetone	-	1.33E+00	-	-	-	-	-	-
Dimethylamine	-	1.01E+00	-	-	-	-	-	-
Propane	-	-	8.80E+00	-	-	-	-	-
Hydrochloric acid	-	-	7.30E+00	-	-	-	-	-
Acetonitrile	-	-	1.60E-01	-	-	-	-	-
Silicon	-	-	-	1.70E-01	-	-	-	-
Ethanol	_	-	-	9.80E-01	3.10E-01	-	-	-
Ethylene glycol	_	-	-	-	1.70E-02	-	-	-
Ethylene	_	-	-	-	8.50E-01	-	-	-
Silver	-	-	-	-	3.40E-05	-	-	-
Phenol	-	-	-	-	-	2.10E-01	-	-

Hydrogen peroxide	-	-	-	-	-	8.00E-02	-	-
Butanediol	-	-	-	-	-	_	1.06E+00	-
C22 alkane	-	-	-	-	-	-	-	5.20E-01
C13 alkane	-	-	-	-	-	-	-	3.10E-01
C1 alkane	-	-	-	-	-	-	-	1.10E-01
Hexamethylenediamine	-	-	-	-	-	-	-	1.90E-01

Table S2. Environmental impact indicators, LCIA method used for their calculation, and units of the indicator.

Environmental Impact Indicator	Calculation Method	Unit	Classification
Global Warming Potential (GWP)	IPPC2007 ³¹	Kg CO ₂ Eq.	Ι
Ozone Depletion Potential (ODP)	WMO1999 ³²	Kg CFC-11 Eq.	Ι
Particulate matters (PMP)	RiskPoll model ³³	Kg PM2,5 Eq.	I
Ionising radiation, human health effect model (IR)	ReCiPe2008 ³⁴	Kg U235 Eq.	II
Photochemical ozone formation (POF)	ReCiPe 2008 ³⁵	Kg NMVOC Eq.	II
Acidification Potential (AC), accumulated exceedance.	36,37	Mole of H+ Eq.	II
Terrestial Eutrophication (EUT), accumulated exceedance	36,37	Mole f N Eq.	II
Resource Depletion Mineral, Fossil, and Renewable (RDM)	CML 2002 ³⁸	Kg Sb Eq.	II
Aquatic freshwater Eutrophication (EUF)	ReCiPe2008 ³⁹	Kg of N Eq.	II
Aquatic marine Eutrophication (EUM)	ReCiPe2008 ³⁹	Kg of N Eq.	II
Human Toxicity Potential, Cancer ffects (HTC)		Comparative Toxic Unit for Human Health (CTUh)	II/III
Human Toxicity Potential, Non Cancer Effects (HTNC)	UseTox ⁴⁰	CTUh	II/III
Ecotoxicity freshwater (ECFW)	UseTox ⁴⁰	Comparative Toxic Unit for ecosystems (CTUe)	II/III
Resource Depletion Water	41	m³ Eq.	III

 Table S3. Environmental impact indicators for the synthesis of conventional seed layer

Environmental Impact						Polyacrilic	Ethylene	
Indicator	TEOS	ТРАОН	Energy	Silica	Water	acid	glycol	TOTAL
GWP (kg CO2 Eq.)	1.61E+01	8.84E+00	2.34E+01	3.85E-01	2.44E-01	1.41E+01	3.32E+00	6.64E+01
ODP (kg CFC-11 Eq.)	1.88E-10	5.53E-11	2.52E-11	1.38E-12	3.28E-12	1.47E-10	4.66E-11	4.66E-10
PMP (kg PM2,5-Eq.)	2.19E-03	1.16E-03	8.94E-04	1.41E-02	3.37E-05	2.29E-03	4.52E-04	2.12E-02
IR (kBq U235 Eq.)	1.30E+00	5.66E-01	2.76E-01	3.38E-02	3.83E-02	1.44E+00	4.62E-01	4.11E+00
POF (kg NMVOC Eq.)	3.40E-02	1.95E-02	2.10E-02	5.23E-04	4.82E-04	4.50E-02	8.76E-03	1.29E-01
AC (Mole of H+ Eq.)	4.21E-02	2.65E-02	1.96E-02	6.49E-04	6.38E-04	5.47E-02	1.06E-02	1.55E-01
EUT (Mole of N Eq.)	1.04E-01	5.49E-02	7.14E-02	2.09E-03	2.01E-03	1.72E-01	2.39E-02	4.30E-01
RDM (kg Sb Eq.)	1.76E-05	1.31E-05	8.13E-06	9.13E-07	3.78E-07	1.90E-05	5.95E-06	6.51E-05
EUF (Mole of P Eq.)	4.92E-05	2.41E-05	1.74E-06	1.24E-06	9.18E-06	2.36E-05	1.36E-05	1.23E-04
EUM (Mole of N Eq.)	9.73E-03	5.91E-03	6.48E-04	2.09E-04	2.23E-04	1.01E-02	2.32E-03	2.91E-02
HTC (CTUh)	9.27E-08	1.46E-07	4.19E-09	2.57E-10	9.39E-10	1.47E-07	4.65E-08	4.38E-07
HTNC (CTUh)	8.65E-07	9.53E-07	1.65E-08	-3.50E-09	5.36E-09	5.89E-07	1.71E-07	2.60E-06
ECFW (CTUe)	2.48E+00	3.06E+00	1.72E-01	3.60E-03	2.87E-02	3.22E+00	1.02E+00	9.98E+00
RDW (m³ Eq.)	3.50E-01	1.30E-01	3.90E-02	3.17E-02	2.31E-02	2.55E-01	9.75E-02	9.26E-01

Table S4. Environmental impact indicators for the synthesis of nanosheets seed layer

Environmental Impact								
Indicator	Surfactant	Toluene	Ethanol	Polystyrene	Water	Energy	TEOS	TOTAL
GWP (kg CO2 Eq.)	8.30E-01	2.68E+01	1.10E-01	9.00E+00	9.07E-04	1.05E+01	2.17E+00	4.94E+01
ODP (kg CFC-11 Eq.)	4.78E-13	7.73E-12	8.36E-14	1.46E-11	1.22E-14	1.14E-11	2.52E-11	5.95E-11
PMP (kg PM2,5-Eq.)	6.32E-05	3.09E-03	6.33E-06	7.04E-04	1.25E-07	3.65E-04	2.95E-04	4.52E-03
IR (kBq U235 Eq.)	7.20E-03	1.55E-01	1.09E-03	2.96E-01	1.42E-04	1.24E-01	1.74E-01	7.58E-01
POF (kg NMVOC Eq.)	1.36E-03	5.00E-02	1.69E-04	1.59E-02	1.79E-06	9.48E-03	4.57E-03	8.15E-02
AC (Mole of H+ Eq.)	1.32E-03	7.34E-02	1.70E-04	1.77E-02	2.37E-06	8.85E-03	5.65E-03	1.07E-01
EUT (Mole of N Eq.)	3.46E-03	1.28E-01	4.65E-04	4.54E-02	7.47E-06	3.22E-02	1.39E-02	2.24E-01
RDM (kg Sb Eq.)	5.45E-07	2.70E-05	5.70E-08	7.27E-06	1.40E-09	3.66E-06	2.37E-06	4.09E-05
EUF (Mole of P Eq.)	8.67E-07	3.22E-05	2.93E-07	1.60E-05	3.41E-08	7.83E-07	6.61E-06	5.68E-05
EUM (Mole of N Eq.)	3.56E-04	1.20E-02	4.46E-05	4.33E-03	8.29E-07	2.92E-03	1.31E-03	2.09E-02
HTC (CTUh)	2.10E-08	7.97E-07	6.95E-10	9.01E-08	3.49E-12	1.88E-09	1.25E-08	9.23E-07
HTNC (CTUh)	1.62E-06	2.71E-06	2.46E-09	3.08E-07	1.99E-11	7.40E-09	1.16E-07	4.76E-06
ECFW (CTUe)	1.79E-01	1.63E+01	1.55E-02	1.94E+00	1.06E-04	7.73E-02	3.33E-01	1.88E+01
RDW (m³ Eq.)	6.84E-03	1.36E-01	6.66E-04	1.08E-01	8.57E-05	1.75E-02	4.70E-02	3.16E-01

Table S5- Coefficients of variation [%] of environmental impact indicators for the Monte Carlo analysis of the conventional seeds layer synthesis (only standard deviations ≥ 0.3 % are shown)

Environmental Impact Indicator	TEOS	ТРАОН	Silica	Energy	Polyacrylic acid
GWP	2.06	0.65	-	1.87	1.11
ODP	2.45	0.78	-	-	1.98
PMP	0.91	0.51	3.51	0.66	1.41
IR	2.42	0.78	-	-	2.01
POC	1.84	0.78	-	0.93	1.95
AC	1.92	0.88	-	0.71	1.99
EUT	1.67	0.66	-	0.99	2.22
RDM	2.04	0.99	-	0.58	1.69
EUF	2.88	1.06	-	0.03	1.05
EUM	1.94	0.88	-	1.11	1.60
HTC	1.45	1.73	-	0.06	1.88
HTNC	2.29	1.93	-	0.04	1.25
ECFW	1.71	1.60	-	0.09	1.80
RDW	2.79	0.79	-	0.05	1.54

Table S6- Coefficients of variation [%] of environmental impact indicators for the Monte Carlo analysis of the nanosheets seed layer synthesis (only standard deviations ≥ 0.3 % are shown)

Environmental			
Impact Indicator	Toluene	Polystyrene	TEOS
GWP	2.83	0.98	0.30
ODP	1.92	2.01	1.45
PMP	3.44	0.88	0.51
IR	1.50	2.27	1.54
POC	3.22	1.11	0.31
AC	3.62	0.95	0.32
EUT	3.02	1.12	0.39
RDM	3.67	0.96	0.35
EUF	3.22	1.48	0.40
EUM	3.02	1.14	0.30
HTC	4.72	0.55	0.08
HTNC	3.06	0.35	0.07
ECFW	4.73	0.58	0.06
RDW	2.61	1.81	0.41

Table S7. Environmental impact indicators for the solution-based sol-gel secondary growth

Environmental Impact						
Indicator	TEOS	ТРАОН	Ethanol	Energy	Water	TOTAL
GWP (kg CO2 Eq.)	1.51E+03	8.31E+02	3.86E+02	5.32E+02	9.06E+00	3.27E+03
ODP (kg CFC-11 Eq.)	1.76E-08	5.20E-09	2.92E-10	5.73E-10	1.07E-10	2.38E-08
PMP (kg PM2,5-Eq.)	2.06E-01	1.09E-01	2.21E-02	1.84E-02	1.28E-03	3.57E-01
IR (kBq U235 Eq.)	1.22E+02	5.32E+01	3.81E+00	6.28E+00	1.30E+00	1.86E+02
POF (kg NMVOC Eq.)	3.20E+00	1.83E+00	5.91E-01	4.78E-01	1.84E-02	6.12E+00
AC (Mole of H+ Eq.)	3.95E+00	2.49E+00	5.93E-01	4.46E-01	2.37E-02	7.50E+00
EUT (Mole of N Eq.)	9.73E+00	5.16E+00	1.63E+00	1.62E+00	7.68E-02	1.82E+01
RDM (kg Sb Eq.)	1.65E-03	1.23E-03	1.99E-04	1.85E-04	1.55E-05	3.29E-03
EUF (Mole of P Eq.)	4.62E-03	2.27E-03	1.02E-03	3.96E-05	2.60E-04	8.21E-03
EUM (Mole of N Eq.)	9.14E-01	5.55E-01	1.56E-01	1.47E-01	7.96E-03	1.78E+00
HTC (CTUh)	8.70E-06	1.37E-05	2.43E-06	9.52E-08	3.17E-08	2.50E-05
HTNC (CTUh)	8.12E-05	8.96E-05	8.60E-06	3.75E-07	1.75E-07	1.80E-04
ECFW (CTUe)	2.33E+02	2.88E+02	5.43E+01	3.90E+00	9.02E-01	5.80E+02
RDW (m³ Eq.)	3.29E+01	1.22E+01	2.33E+00	8.85E-01	9.17E-01	4.92E+01

Table S8. Environmental impact indicators for the gel-less (gel-free) secondary growth

Environmental Impact			Brower	
Indicator	ТРАОН	Energy	Water	TOTAL
GWP (kg CO2 Eq.)	3.88E+02	1.08E+03	1.06E+01	1.48E+03
ODP (kg CFC-11 Eq.)	2.43E-09	1.16E-09	1.25E-10	3.72E-09
PMP (kg PM2,5-Eq.)	5.10E-02	3.74E-02	1.50E-03	8.99E-02
IR (kBq U235 Eq.)	2.48E+01	1.27E+01	1.53E+00	3.90E+01
POF (kg NMVOC Eq.)	8.56E-01	9.71E-01	2.16E-02	1.85E+00
AC (Mole of H+ Eq.)	1.16E+00	9.06E-01	2.78E-02	2.09E+00
EUT (Mole of N Eq.)	2.41E+00	3.29E+00	9.01E-02	5.79E+00
RDM (kg Sb Eq.)	5.77E-04	3.75E-04	1.82E-05	9.70E-04
EUF (Mole of P Eq.)	1.06E-03	8.03E-05	3.05E-04	1.45E-03
EUM (Mole of N Eq.)	2.59E-01	2.98E-01	9.34E-03	5.66E-01
HTC (CTUh)	6.41E-06	1.93E-07	3.72E-08	6.64E-06
HTNC (CTUh)	4.18E-05	7.61E-07	2.06E-07	4.28E-05
ECFW (CTUe)	1.34E+02	7.92E+00	1.06E+00	1.43E+02
RDW (m³ Eq.)	5.71E+00	1.80E+00	1.08E+00	8.59E+00

Table S9- Coefficients of variation [%] of environmental impact indicators for the Monte Carlo analysis of the solution-based sol-gel and for the gel-less (gel-free) secondary growths (only standard deviations ≥ 0.3 % are shown)

Environmental	Solution-based	d sol-gel	Gel-less (gel-f	ree)
Impact Indicator	TEOS	ТРАОН	ТРАОН	Energy
GWP	3.06	1.30	1.23	4.21
ODP	3.94	1.72	5.23	-
PMP	3.83	1.40	2.71	2.68
IR	3.92	1.72	4.98	-
POC	3.02	1.75	2.26	3.16
AC	3.08	1.92	2.77	2.63
EUT	3.06	1.65	1.96	3.45
RDM	3.11	2.05	3.20	2.20
EUF	3.26	1.63	3.61	-
EUM	2.95	1.81	2.16	3.23
HTC	1.98	3.22	5.22	-
HTNC	2.56	2.93	5.28	-
ECFW	2.29	2.90	5.04	0.35
RDW	3.93	1.51	4.14	-

Table S10. Environmental impact indicators for the Piranha treated nanosheets method

Environmental Impact				Hydrogen			Sulphuric	
Indicator	DQAS	TEOS	Ethanol	peroxide	Energy	Water	acid	TOTAL
GWP (kg CO2 Eq.)	4.14E+00	1.08E+01	5.50E-01	1.32E+00	8.98E+00	8.93E-03	2.25E+00	2.81E+01
ODP (kg CFC-11 Eq.)	2.38E-12	1.26E-10	4.16E-13	1.67E-12	9.67E-12	1.05E-13	2.34E-11	1.64E-10
PMP (kg PM2,5-Eq.)	3.16E-04	1.47E-03	3.16E-05	5.30E-05	3.11E-04	1.26E-06	2.76E-03	4.95E-03
IR (kBq U235 Eq.)	3.59E-02	8.72E-01	5.43E-03	3.96E-02	1.06E-01	1.28E-03	2.26E-01	1.29E+00
POF (kg NMVOC Eq.)	6.77E-03	2.29E-02	8.42E-04	1.25E-03	8.07E-03	1.81E-05	8.76E-03	4.86E-02
AC (Mole of H+ Eq.)	6.57E-03	2.83E-02	8.45E-04	1.41E-03	7.53E-03	2.33E-05	6.01E-02	1.05E-01
EUT (Mole of N Eq.)	1.73E-02	6.96E-02	2.32E-03	4.43E-03	2.74E-02	7.56E-05	1.38E-02	1.35E-01
RDM (kg Sb Eq.)	2.72E-06	1.18E-05	2.84E-07	1.26E-06	3.12E-06	1.52E-08	3.39E-06	2.26E-05
EUF (Mole of P Eq.)	4.33E-06	3.30E-05	1.46E-06	5.03E-06	6.67E-07	2.56E-07	7.19E-06	5.20E-05
EUM (Mole of N Eq.)	1.78E-03	6.54E-03	2.22E-04	4.38E-04	2.48E-03	7.84E-06	1.35E-03	1.28E-02
HTC (CTUh)	1.05E-07	6.23E-08	3.47E-09	2.98E-09	1.60E-09	3.12E-11	4.39E-08	2.19E-07
HTNC (CTUh)	8.07E-06	5.81E-07	1.23E-08	2.76E-07	6.30E-09	1.73E-10	1.70E-07	9.12E-06
ECFW (CTUe)	8.92E-01	1.67E+00	7.74E-02	2.19E-02	6.58E-02	8.88E-04	9.76E-01	3.70E+00
RDW (m³ Eq.)	3.41E-02	2.35E-01	3.32E-03	3.47E-02	1.49E-02	9.03E-04	3.93E-02	3.62E-01

Table S11- Coefficients of variation [%] of environmental impact indicators for the Monte Carlo analysis of the Piranha treated nanosheets method (only standard deviations ≥ 0.3 % are shown)

Environmental Impact Indicator	TEOS	H ₂ SO ₄	Energy	DQAS
GWP	2.53	0.41	1.75	0.72
ODP	4.21	1.04	-	-
PMP	1.50	3.01	0.37	0.41
IR	4.22	0.92	-	-
POC	2.67	1.10	1.03	0.71
AC	1.50	3.26	0.42	0.41
EUT	2.88	0.59	1.30	0.61
RDM	3.12	0.83	0.67	0.59
EUF	3.69	0.71	-	0.42
EUM	2.87	0.52	1.25	0.68
HTC	1.61	1.02	-	0.75
HTNC	0.35	-	-	5.07
ECFW	2.57	1.51	-	1.38
RDW	3.84	0.63	-	0.61

Table S12. Environmental impact indicators for the synthesis of silica support

Environmental Impact					Glass		Polyvinyl	
Indicator	TEOS	Ethanol	Ammonia	Energy	wool	Water	alcohol	TOTAL
GWP (kg CO2 Eq.)	2.46E+02	1.65E+02	4.92E+01	2.14E+03	8.76E+03	6.48E+00	3.26E+01	1.14E+04
ODP (kg CFC-11 Eq.)	2.87E-09	1.25E-10	4.12E-11	1.22E-09	1.14E-07	7.62E-11	1.77E-10	1.19E-07
PMP (kg PM2,5-Eq.)	3.35E-02	9.44E-03	9.56E-04	3.93E-02	7.60E+00	9.16E-04	2.50E-03	7.69E+00
IR (kBq U235 Eq.)	1.98E+01	1.63E+00	1.41E+00	1.34E+01	9.56E+02	9.31E-01	2.04E+00	9.95E+02
POF (kg NMVOC Eq.)	5.20E-01	2.52E-01	2.06E-02	1.02E+00	2.35E+01	1.32E-02	6.70E-02	2.54E+01
AC (Mole of H+ Eq.)	6.43E-01	2.53E-01	2.31E-02	9.54E-01	6.36E+01	1.69E-02	6.04E-02	6.56E+01
EUT (Mole of N Eq.)	1.58E+00	6.93E-01	6.71E-02	3.47E+00	2.34E+02	5.49E-02	1.68E-01	2.40E+02
RDM (kg Sb Eq.)	2.69E-04	8.49E-05	1.94E-05	3.95E-04	8.93E-01	1.11E-05	4.08E-05	8.93E-01
EUF (Mole of P Eq.)	7.52E-04	4.37E-04	4.71E-05	8.45E-05	1.44E-02	1.86E-04	3.57E-04	1.63E-02
EUM (Mole of N Eq.)	1.49E-01	6.65E-02	2.94E-02	3.14E-01	9.98E+00	5.69E-03	1.80E-02	1.06E+01
HTC (CTUh)	1.42E-06	1.04E-06	7.87E-09	2.03E-07	7.62E-05	2.26E-08	1.51E-07	7.91E-05
HTNC (CTUh)	1.32E-05	3.67E-06	2.14E-08	8.01E-07	2.36E-04	1.25E-07	5.16E-06	2.59E-04
ECFW (CTUe)	3.79E+01	2.32E+01	3.96E-01	8.33E+00	9.65E+02	6.45E-01	5.83E+00	1.04E+03
RDW (m³ Eq.)	5.35E+00	9.92E-01	2.05E-01	1.89E+00	1.56E+02	6.55E-01	7.44E-01	1.66E+02

Table S13. Environmental impact indicators for the synthesis of alumina support

Environmental Impact			
Indicator	Alumina	Energy	TOTAL
GWP (kg CO2 Eq.)	8.61E+03	9.01E+02	9.51E+03
ODP (kg CFC-11 Eq.)	1.60E-08	9.70E-10	1.70E-08
PMP (kg PM2,5-Eq.)	1.68E+00	3.12E-02	1.71E+00
IR (kBq U235 Eq.)	1.53E+02	1.06E+01	1.64E+02
POF (kg NMVOC Eq.)	1.48E+01	8.10E-01	1.56E+01
AC (Mole of H+ Eq.)	4.12E+01	7.56E-01	4.19E+01
EUT (Mole of N Eq.)	5.13E+01	2.75E+00	5.40E+01
RDM (kg Sb Eq.)	1.93E-01	3.13E-04	1.93E-01
EUF (Mole of P Eq.)	5.97E-03	6.70E-05	6.03E-03
EUM (Mole of N Eq.)	4.71E+00	2.49E-01	4.96E+00
HTC (CTUh)	2.91E-05	1.61E-07	2.93E-05
HTNC (CTUh)	6.07E-04	6.35E-07	6.07E-04
ECFW (CTUe)	5.26E+02	6.60E+00	5.33E+02
RDW (m³ Eq.)	3.65E+01	1.50E+00	3.80E+01

Table S14. Environmental impact indicators for the synthesis of PBI support

Environmental Impact					
Indicator	DMAc	PBI	Polyethylene	Energy	TOTAL
GWP (kg CO2 Eq.)	6.27E+02	8.70E+02	6.78E+01	5.21E+01	1.62E+03
ODP (kg CFC-11 Eq.)	7.06E-10	1.28E-08	5.20E-10	5.61E-11	1.40E-08
PMP (kg PM2,5-Eq.)	2.10E-02	8.89E-02	7.86E-03	1.80E-03	1.20E-01
IR (kBq U235 Eq.)	1.41E+01	1.15E+02	5.22E+00	6.14E-01	1.35E+02
POF (kg NMVOC Eq.)	5.22E-01	1.29E+00	1.31E-01	4.68E-02	1.99E+00
AC (Mole of H+ Eq.)	5.34E-01	1.75E+00	1.53E-01	4.37E-02	2.48E+00
EUT (Mole of N Eq.)	1.43E+00	4.55E+00	3.61E-01	1.59E-01	6.50E+00
RDM (kg Sb Eq.)	3.06E-04	2.04E-03	7.68E-05	1.81E-05	2.44E-03
EUF (Mole of P Eq.)	5.79E-04	1.46E-03	1.21E-04	3.87E-06	2.16E-03
EUM (Mole of N Eq.)	2.82E-01	4.51E-01	3.47E-02	1.44E-02	7.82E-01
HTC (CTUh)	1.09E-06	3.07E-06	6.64E-07	9.31E-09	4.84E-06
HTNC (CTUh)	4.28E-06	1.44E-05	2.36E-06	3.66E-08	2.11E-05
ECFW (CTUe)	2.63E+01	6.83E+01	1.45E+01	3.82E-01	1.09E+02
RDW (m³ Eq.)	2.60E+00	2.09E+01	9.49E-01	8.66E-02	2.45E+01

Table S15- Coefficients of variation [%] of environmental impact indicators for the Monte Carlo analysis of the synthesis of different supports (only standard deviations ≥ 0.3 % are shown)

	Silica	Alumina	PBI	PBI		HF Alumina	
Environmental Impact Indicator	Glass wool	Alumina	PBI	DMAc	Alumina	N-methyl-2- pyrrolidone	
GWP	4.80	5.24	2.81	2.15	1.38	4.37	
ODP	5.50	5.77	4.67	0.30	0.96	4.69	
PMP	5.45	5.67	3.92	0.71	2.21	3.41	
IR	5.50	5.75	4.61	0.44	1.05	4.57	
POC	5.24	5.48	3.36	1.48	2.00	3.62	
AC	5.50	5.68	3.69	1.15	2.37	3.22	
EUT	5.51	5.47	3.59	0.68	2.04	3.57	
RDM	5.16	5.76	4.39	0.70	4.75	0.50	
EUF	5.03	5.75	3.59	1.48	-	5.78	
EUM	5.34	5.48	2.96	2.01	1.76	3.91	
HTC	5.43	5.74	3.25	1.36	2.05	3.42	
HTNC	5.14	5.76	3.44	1.24	4.24	0.94	
ECFW	5.21	5.70	3.20	1.38	1.09	4.62	
RDW	5.38	5.73	4.60	0.45	0.36	5.50	

Table S16. Environmental impact indicators for the synthesis of alumina hollow fiber support

Environmental Impact			N-methyl-2-			
Indicator	Alumina	Polysulfone	pyrrolidone	Energy	Water	TOTAL
GWP (kg CO2 Eq.)	1.29E+02	3.24E+01	4.84E+02	4.46E+01	3.63E-01	6.91E+02
ODP (kg CFC-11 Eq.)	2.40E-10	3.02E-10	5.19E-10	4.80E-11	4.27E-12	1.11E-09
PMP (kg PM2,5-Eq.)	2.53E-02	4.84E-03	4.81E-02	1.54E-03	5.13E-05	7.98E-02
IR (kBq U235 Eq.)	2.30E+00	2.78E+00	1.18E+01	5.26E-01	5.21E-02	1.75E+01
POF (kg NMVOC Eq.)	2.22E-01	6.65E-02	5.08E-01	4.01E-02	7.37E-04	8.38E-01
AC (Mole of H+ Eq.)	6.18E-01	1.04E-01	1.05E+00	3.74E-02	9.49E-04	1.81E+00
EUT (Mole of N Eq.)	7.70E-01	2.02E-01	1.62E+00	1.36E-01	3.08E-03	2.74E+00
RDM (kg Sb Eq.)	2.90E-03	4.42E-05	3.18E-04	1.55E-05	6.20E-07	3.27E-03
EUF (Mole of P Eq.)	8.95E-05	8.58E-05	3.46E-03	3.32E-06	1.04E-05	3.65E-03
EUM (Mole of N Eq.)	7.07E-02	1.91E-02	1.89E-01	1.23E-02	3.19E-04	2.92E-01
HTC (CTUh)	4.37E-07	2.80E-07	9.03E-07	7.97E-09	1.27E-09	1.63E-06
HTNC (CTUh)	9.11E-06	1.97E-06	2.83E-06	3.14E-08	7.02E-09	1.39E-05
ECFW (CTUe)	7.90E+00	5.92E+00	4.04E+01	3.27E-01	3.61E-02	5.46E+01
RDW (m³ Eq.)	5.47E-01	8.81E-01	1.00E+01	7.42E-02	3.67E-02	1.16E+01

References

- (1) Kroschwitz, J. I.; Howe-Grant, M.; *Kirk-Othmer Encyclopedia of Chemical Technology*; Wiley: New Jersey, 2014.
- (2) Simmler, W. Silicon Compunds, Inorganic. In *Ullmann's Encycl. Ind. Chem.;* Wiley: New Jersey, 2010.
- (3) Lawrence, S. A. *Amines: Synthesis, Properties and Applications.*; Cambridge University Press: Cambridge, 2005.
- (4) Kricheldorf, H. R. *Handbook of Polymer Synthesis*; New York: Marcel Dekker, 2005.
- (5) Gehatia, M.; Wiff, D. R. Molecular Weight Distribution of Polybenzimidazole. A Regularizable Ill-Posed Problem. *J. Chem. Phys.* **2003**, *57*, 1070-1074.
- (6) Druin, M. L.; Oringer, K. Synthesis of Pure 3,3'-Diaminobenzidine. US Patent. 3943175, March 9, 1973.
- (7) Schwenecke, H.; Mayer, D. Benzidine and Benzidine Derivatives. In *Ullmann's Encycl. Ind. Chem.*; Wiley: New Jersey, 2010.
- (8) Markofsky, S. B. Nitrocompounds, Aliphatic. *Ullmann's Encycl. Ind. Chem.*; Wiley: New Jersey, 2011.
- (9) Beck, U.; Löser, E. Chlorinated Benzenes and Other Nucleous-Chlorinated Aromatic Hydrocarbons. In *Ullmann's Encycl. Ind. Chem.*; Wiley: New Jersey, 2010.
- (10) Wildermuth, E.; Stark, H.; Friedrich, G.; Ebenhöch, F. L.; Kühborth, B.; Silver, J.; Rituper, R. Iron Compounds. In *Ullmann's Encycl. Ind. Chem.;* Wiley: New Jersey, 2010.
- (11) Lorz, P. M.; Towae, F. W.; Rudolf Jäckh, W. E.; Bhargava, N.; Hillesheim, W. Phthalic Acid and Derivatives. In *Ullmann's Encycl. Ind. Chem.*; Wiley: New Jersey, 2010.
- (12) Bauer, G.; Güther, V.; Hess, H.; Otto, A.; Roidl, O.; Roller, H.; Sattelberger, S. Vanadium and Vanadium Compounds. In *Ullmann's Encycl. Ind. Chem.*; Wiley: New Jersey, 2010.
- (13) Vanitec. Vanadium Sources. http://vanitec.org/vanadium/making-vanadium (accessed March 16, 2018).
- (14) Fabri, J.; Graeser, U.; Simo, T. A. Xylenes. In *Ullmann's Encycl. Ind. Chem.*; Wiley: New Jersey, 2010.
- (15) Cheung, H.; Tanke, R. S.; Paul Torrence, G. Acetic Acid. In *Ullmann's Encycl. Ind. Chem.*; Wiley: New Jersey, 2010.
- (16) Hayes, K. S. Industrial Processes for Manufacturing Amines. *Appl. Catal. A-Gen.* **2001**, 221, 187–195.
- (17) Rebsdat, S.; Mayer, D. Ethylene Glycol. In *Ullmann's Encycl. Ind. Chem.*; Wiley: New Jersey, 2010.
- (18) Rebsdat, S.; Mayer, D. Ethylene Oxide. In *Ullmann's Encycl. Ind. Chem.;* Wiley: New Jersey, 2010.
- (19) Parker, D.; Bussink, J.; van de Grampel, H.T.; Wheatley, G.W.; Dorf, E.-U.; Ostlinning, E.; Reinking, K.; Schubert, F. Polymers, High-Temperature. In *Ullmann's Encycl. Ind. Chem.*; Wiley: New Jersey, 2012.
- (20) Harreus, A.; Backes, R.; Eichler, J.-O.; Feuerhake, R.; Jäkel, C.; Mahn, U.; Pinkos, R.; Vogelsang, R. 2-Pyrrolidone. In *Ullmann's Encycl. Ind. Chem.*; Wiley: New Jersey, 2011.
- (21) Wolfgang, S.; Jürgen, S.; Roland, R.; Hartmut, H. Butyrolactone. In *Ullmann's Encycl. Ind. Chem.;* Wiley: New Jersey, 2000.
- (22) Choi, M.; Na, K.; Kim, J.; Sakamoto, Y.; Terasaki, O.; Ryoo, R. Stable Single-Unit-Cell Nanosheets of Zeolite MFI as Active and Long-Lived Catalysts. *Nature* **2009**, *461*, 246–

- 249.
- (23) Elyassi, B.; Jeon, M. Y.; Tsapatsis, M.; Narasimharao, K.; Sulaiman, N. M. N.; Al-Thabaiti, S. Ethanol/Water Mixture Pervaporation Performance of b-Oriented Silicalite-1 Membranes Made by Gel-Free Secondary Growth. *AIChE J.* **2016**, *62*, 556-563.
- (24) Varoon, K.; Zhang, X.; Elyassi, B.; Brewer, D. D.; Gettel, M.; Kumar, S.; Lee, J. A.; Maheshwari, S.; Mittal, A.; Sung, C. Y.; et al. Dispersible Exfoliated Zeolite Nanosheets and Their Application as a Selective Membrane. *Science* **2011**, *334*, 72–75.
- (25) Agrawal, K. V.; Topuz, B.; Pham, T. C. T.; Nguyen, T. H.; Sauer, N.; Rangnekar, N.; Zhang, H.; Narasimharao, K.; Basahel, S. N.; Francis, L. F.; et al. Oriented MFI Membranes by Gel-Less Secondary Growth of Sub-100 Nm MFI-Nanosheet Seed Layers. *Adv. Mater.* **2015,** *27*, 3243–3249.
- (26) Zhang, H.; Xiao, Q.; Guo, X.; Li, N.; Kumar, P.; Rangnekar, N.; Jeon, M. Y.; Al-Thabaiti, S.; Narasimharao, K.; Basahel, S. N.; et al. Open-Pore Two-Dimensional MFI Zeolite Nanosheets for the Fabrication of Hydrocarbon-Isomer-Selective Membranes on Porous Polymer Supports. *Angew. Chem. Int. Edit.* 2016, 55, 7184–7187.
- (27) Varoon, K.; Topuz, B.; Jiang, Z.; Nguenkam, K.; Elyassi, B.; Francis, L. F.; Tsapatsis, M.; Navarro, M. Solution-Processable Exfoliated Zeolite Nanosheets Purified by Density Gradient Centrifugation. *AIChE J.* **2013**, *59*, 3458-3467.
- (28) Choi, J.; Ghosh, S.; King, L.; Tsapatsis, M. MFI Zeolite Membranes from A- and Randomly Oriented Monolayers. *Adsorption* **2006**, *12*, 339–360.
- (29) European Aluminium Association, Environmental profile report, Life-Cycle inventory data for aluminium production and transformation processes in Europe February 2018. https://www.european-aluminium.eu/resource-hub/environmental-profile-report-2018/. (accessed March 16, 2018).
- (30) Shao, J.; Zhan, Z.; Li, J.; Wang, Z.; Li, K.; Yan, Y. Zeolite NaA Membranes Supported on Alumina Hollow Fibers: Effect of Support Resistances on Pervaporation Performance. *J. Membrane Sci.* **2014**, *451*, 10–17.
- (31) IPCC, 2007: Climate Change 2007: Synthesis Report. Contribution of Working Groups I, II and III to the Fourth Assessment Report of the Intergovernmental Panel on Climate Change. Pachauri, R.K., and Reisinger, A., Eds. IPCC, Geneva, Switzerland; 2007.
- (32) US Department of Commerce, World Meteorological Organization Global Ozone Research and Monitoring Project. Scientific Assessment of Ozone Depletion. 1998.
- (33) Greco, S. L.; Wilson, A. M.; Spengler, J. D.; Levy, J. I. Spatial Patterns of Mobile Source Particulate Matter Emissions-to-Exposure Relationships across the United States. *Atmos. Environ.* **2007**, *41*, 1011–1025.
- (34) Frischknecht, R.; Braunschweig, A.; Hofstetter, P.; Suter, P. Human Health Damages Due to Ionising Radiation in Life Cycle Impact Assessment. *Environ. Impact Assess.* **2000**, 20, 159–189.
- (35) van Zelm, R.; Huijbregts, M. A. J.; den Hollander, H. A.; van Jaarsveld, H. A.; Sauter, F. J.; Struijs, J.; van Wijnen, H. J.; van de Meent, D. European Characterization Factors for Human Health Damage of PM10 and Ozone in Life Cycle Impact Assessment. *Atmos. Environ.* **2008**, *42*, 441–453.
- (36) Seppälä, J.; Posch, M.; Johansson, M.; Hettelingh, J.-P. Country-Dependent Characterisation Factors for Acidification and Terrestrial Eutrophication Based on Accumulated Exceedance as an Impact Category Indicator (14 Pp). *Int. J. Life Cycle Ass.* **2006,** *11,* 403–416.

- (37) Posch, M.; Seppälä, J.; Hettelingh, J.-P.; Johansson, M.; Margni, M.; Jolliet, O. The Role of Atmospheric Dispersion Models and Ecosystem Sensitivity in the Determination of Characterisation Factors for Acidifying and Eutrophying Emissions in LCIA. *Int. J. Life Cycle Ass.* **2008**, *13*, 477–486.
- (38) Guinee, J. B., Ed. Handbook on Life Cycle Assessment Operational Guide to the ISO Standards; Springer: The Netherlands, 2002.
- (39) Goedkoop, M.; Heijungs, R.; Huijbregts, M.; De Schryver, A.; Struijs, J.; Van Zelm, R. ReCiPe 2008 First Edition Report I: Characterisation. https://www.rivm.nl/dsresource?objectid=8ed17c8e-a370-437f-afc7-3004b6cce2bc (accessed March 16, 2018).
- (40) Rosenbaum, R. K.; Bachmann, T. M.; Gold, L. S.; Huijbregts, M. A. J.; Jolliet, O.; Juraske, R.; Koehler, A.; Larsen, H. F.; MacLeod, M.; Margni, M.; et al. USEtox—the UNEP-SETAC Toxicity Model: Recommended Characterisation Factors for Human Toxicity and Freshwater Ecotoxicity in Life Cycle Impact Assessment. *Int. J. Life Cycle Ass.* 2008, 13, 532–546.
- (41) Frischknecht, R.; Steiner, R.; Jungbluth, N. The Ecological Scarcity Method Eco-Factors 2006 A Method for Impact Assessment in LCA (Methode Der Ökologischen Knappheit Ökofaktoren 2006 Methode Für Die Wirkungsabschätzung in Ökobilanzen). https://www.bafu.admin.ch/bafu/en/home/topics/economy-consumption/economy-and-consumption-publications/publications-economy-and-consumption/ecological-scarcity-ethod-eco-factors-2006.html. (accessed March 16, 2018).